

SEA GRANT

Dissertation Series

UNIVERSITY OF SOUTHERN CALIFORNIA
Institute for Marine and Coastal Studies
University Park, Los Angeles, CA 90007





The Institute for Marine and Coastal Studies was founded by the University of Southern California in 1975 to be the institutional framework for its marine programs, many of which had been in operation since the early 1900s. The Institute promotes basic and applied research, as well as training in marine studies; sponsors workshops, conferences and extension courses; and produces reports and publications based on Institute-sponsored research. The work of the Institute takes place throughout the Southern California region--at USC's University Park campus, on several research vessels, at the research facilities located at the Port of Los Angeles and the Catalina Marine Science Center on Santa Catalina Island.

A part of the Institute is the Sea Grant program, funded by the National Oceanic and Atmospheric Administration, Department of Commerce. Each year, the USC Sea Grant program supports one or more research projects in each of the following areas: socio-economic systems, living marine resources, non-living marine resources, coastal engineering, marine education and advisory services.

VARIABILITY IN TEMPERATURE IN COASTAL
WATERS NEAR THE PALOS VERDES PENINSULA BETWEEN
JANUARY AND MAY 1985

John Alexander Steele

USCSG-TD-01-87

LOAN COPY ONLY

CIRCULATING COPY
Sea Grant Depository

John Alexander Steele
1985-86 Trainee for R/EQ-40

This work is the result of a research project sponsored by the University of Southern California's Sea Grant Institutional Program, Institute for Marine and Coastal Studies. Funding was provided for R/EQ-40 by the National Sea Grant College Program, National Oceanic and Atmospheric Administration, Department of Commerce, and the State of California.

This document is published and distributed by:

USC Sea Grant Institutional Program
Institute for Marine and Coastal Studies
University of Southern California
University Park
Los Angeles, CA 90089-0341

2/87

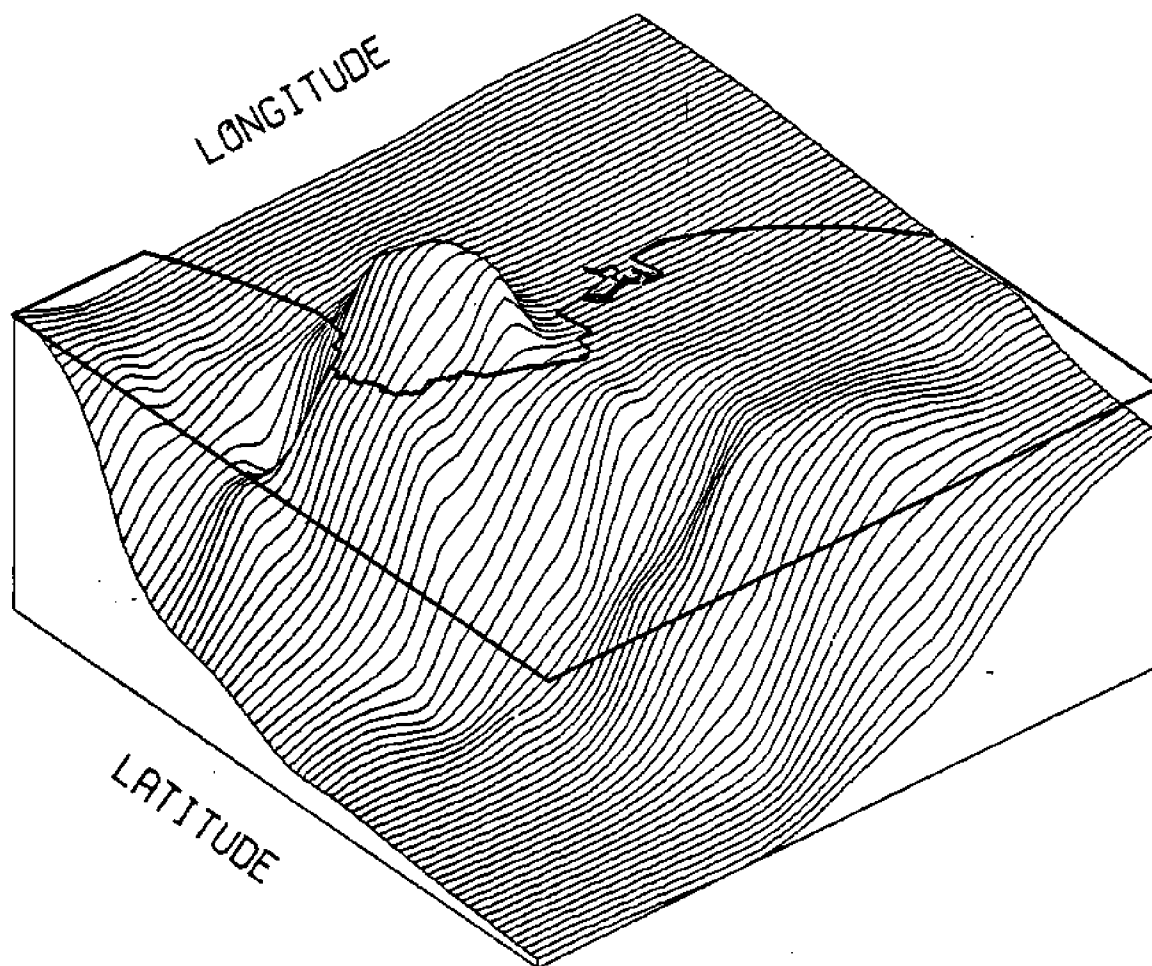
NATIONAL SEA GRANT DEPOSITORY
PAUL HENRY BUILDING
UNIVERSITY OF CALIFORNIA, LAFAYETTE CAMPUS
LAFAYETTE, CA 94502-0282

VARIABILITY IN TEMPERATURE IN COASTAL WATERS
NEAR THE PALOS VERDES PENINSULA BETWEEN JANUARY
AND MAY 1985

by

John Alexander Steele

PALOS VERDES PENINSULA



VARIABILITY IN TEMPERATURE IN COASTAL WATERS
NEAR THE PALOS VERDES PENINSULA BETWEEN JANUARY
AND MAY 1985

by
John Alexander Steele

A Thesis Presented to the
FACULTY OF THE GRADUATE SCHOOL
UNIVERSITY OF SOUTHERN CALIFORNIA
In Partial Fulfillment of the
Requirements for the Degree
MASTER OF SCIENCE
(Geological Sciences)

December 1986

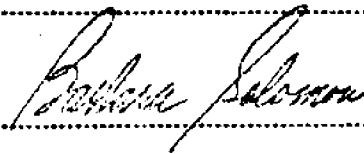
UNIVERSITY OF SOUTHERN CALIFORNIA
THE GRADUATE SCHOOL
UNIVERSITY PARK
LOS ANGELES, CALIFORNIA 90007

This thesis, written by

John Alexander Steele

*under the direction of his...Thesis Committee,
and approved by all its members, has been pre-
sented to and accepted by the Dean of The
Graduate School, in partial fulfillment of the
requirements for the degree of*

Master of Science



Dean

Date September 2, 1986

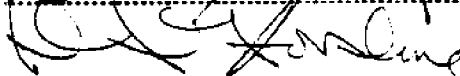
THESIS COMMITTEE



Chairman



Co-chairman



ACKNOWLEDGMENTS

I would like to thank the Sea Grant Program which provided me with support as a Trainee during the last academic year. Sea Grant also helped to make this work possible by supporting the project which collected the data I used. The Los Angeles County Sanitation District provided me with information and also contributed generously to the project. Fellow graduate student Dave Siegel was an important source of information concerning quantitative analysis methods and historical references. My thesis committee including Alan Bratkovich, Burton Jones, Tommy Dickey and Don Gorsline have helped to make this work an educational and enjoyable experience. Tom Dickey first introduced me to this project and offered the opportunity to participate in it. Burton Jones provided assistance with the hardware and software needed to do the work and was a valuable source of ideas and information. Special thanks go to my thesis advisor Alan Bratkovich who guided the development of this thesis in an organized and logical manner.

TABLE OF CONTENTS

	PAGE
Acknowledgments	ii
List of Illustrations	iv
List of Tables	vi
Abstract	vii
1.0 Introduction	1
2.0 Historical Background	8
3.0 Data Base	14
4.0 Analysis	20
5.0 Discussion	74
6.0 Conclusion	94
References	98
Appendix	101

LIST OF ILLUSTRATIONS

Figure	Page
1.1 Map of study area and hydrographic station and mooring locations.....	2
1.2 Expanded map showing location of all sources of data used.....	5
3.1 Time line of 1985 field observations.....	15
3.2 Diagram of mooring arrangement.....	16
4.1 Diagram of Vector Measuring Current Meter (VMCM).....	21
4.2 Comparison of hydrographic vertical profiling measurements with temperature time series	24
4.3 12m temperature time series, filtered time series, and low and high frequency signal components.....	33
4.4 34m temperature time series, filtered time series, and low and high frequency signal components.....	34
4.5 Power spectra of temperature and horizontal current components from mooring time series.....	37
4.6 Seasonal comparison of in autocorrelations of temperature signal.....	38
4.7 Probability density function estimates of temperature for each month January-May 1985. For Temperature at 12m, 34m and the for the averaged temperature gradient between these depths.....	40
4.8 Vertical temperature gradient time series, filtered time series, and low and highfrequency signal components.....	41
4.9 Diurnal temperature cycle and 95% confidence levels for 34m depth time series.....	44
4.10 Diurnal temperature cycle and 95% confidence levels for 12m depth time series.....	45
4.11 Diurnal cycle and 95% confidence levels for temperature gradient timeseries.....	48

Figure	Page
4.12 Diurnal cycles in cross-shelf and alongshelf currents at 12, 23, 34, and 45 meters.....	50
4.13 Vertical monthly averaged profiles of cross-shelf and alongshelf currents with 95% error limits.	53
4.14 Probability distribution of water parcel trajectories using near surface moored current meter data.....	55
4.15 Diurnal cycle of cross-shelf component of local wind.....	57
4.16 Diurnal cycle of alongshelf component of local wind.....	58
4.17 Cross-shelf sections of some of the physical variables and nutrientssampled on the January 23rd hydrographic cruise.....	60
4.18 Principal component results from January 28th cruise data.....	62
4.19 Cross-shelf section of temperature over 120 inch outfall for January 23rd.....	63
4.20 Monthly averaged temperatures and standard deviations at 4m and 19m at the LACSD buoy.....	65
4.21 T/S plot of hydrographic data from January 1985 hydrographic cruises.....	66
4.22 Monthly averaged temperatures and salinities for CalCOFI line 90 station 28, and San Clemente pier-end data.....	68
4.23 Cross-correlations between winds, currents, and temperatures.....	70-71
4.24 Infra-red satellite image of sea surface temperature near Palos Verdes Peninsula, April 1985.....	73
5.1 Monthly averaged temperatures and standard deviations at 12m and 34m.....	75
5.2 Diurnal cycle and 95% confidence levels for sea surface tidal elevation time series.	88

LIST OF TABLES

Table	Page
4.1 Table of temperature values used for linear regression between IACSD BT profiles and VMCM thermistor temperatures.....	26
4.2 Table of scaled values of components of heat budget equation for January 18, 23, 25, and February 11.....	32
4.3 Table of statistics for the 12 and 34 m temperatures and the temperature gradient.....	36
4.4 Table of 12 and 24 hour sine-cosine wave fits to daily averaged cycles.....	46
5.1 Table of diffuser statistics (from Fischer et. al., 1979).....	90

ABSTRACT

During January of 1985 the field work for a Sea Grant/Los Angeles County Sanitation District (SG/LACSD) project began. Data were collected from a set of hydrographic cruises and a mooring consisting of four Vector Measuring Current Meters (VMCM's) deployed from January 14 to May 9, 1985 in 55 m water depth on the outer shelf. This thesis examines the mooring data and some of the hydrographic data as well as wind and sea surface elevation data. Seasonal trends in temperature on the Palos Verdes shelf are found to be anomalous when compared to CalCOFI and pier-end historical data sets. Temperatures at 12 and 34 m are observed to decrease by 2 °C during the first four months of 1985 at 12 m, and by 2.5 °C over the same time interval at 34 m. Historical data sets show a 0.5 - 1.2 °C increase over this period of the year. Estimates of the percent of density variability due to the temperature field made using historical records of temperature and salinity show 50% of wintertime and 90% of summertime density variability may be due to temperature. Spectral analysis shows high spectral energy in the temperature data at diurnal and higher frequencies. Variance levels in the temperature signal at 12 m increase from 0.02 (°C)² in January to 1.7 (°C)² in early May. At 34 m the variance increases from 0.08 to 1.5 (°C)². Autocorrelations show increasing levels of diurnal and semidiurnal variability in each month. Probability density distributions for each month illustrate the spread of temperatures and the temperature gradient from month to month. Averaged 24 hour cycles of winds, currents and temperatures show inter-variable relationships and diurnal and semidiurnal variability.

1.0 INTRODUCTION

The research presented in this thesis is a statistical study of temperature variability in the coastal region near the Los Angeles County Sanitation District (LACSD) sewage outfalls off of Whites Point on the Palos Verdes Peninsula. This study uses time series of temperature data from the University of Southern California (USC) mooring, deployed from January 14 to May 9, 1985, in the study area (see figure 1.1 for mooring location), along with available hydrographic measurements of temperature and salinity, to characterize seasonal temperature stratification conditions using average monthly statistics.

The purpose of this study is to examine the behavior of the temperature field at the shelf break off the Palos Verdes Peninsula. Specific topics that are addressed include; 1) establishing the correlation between our monthly statistics from the mooring and historical data sets from nearby locations, 2) definition of the important scales of variability in the temperature records from the mooring and observations of the changes in higher frequency modes of variability with season, 3) the relationships between winds, currents, surface tides and the temperature field that can be identified using crosscorrelations and averaged daily cycles 4) determination of the percentage of the density stratification at the shelf break which is due to the temperature field, and, 5) implications of the above results regarding the distribution of the waste-water effluent field.

The environment on the Palos Verdes shelf is unique for several

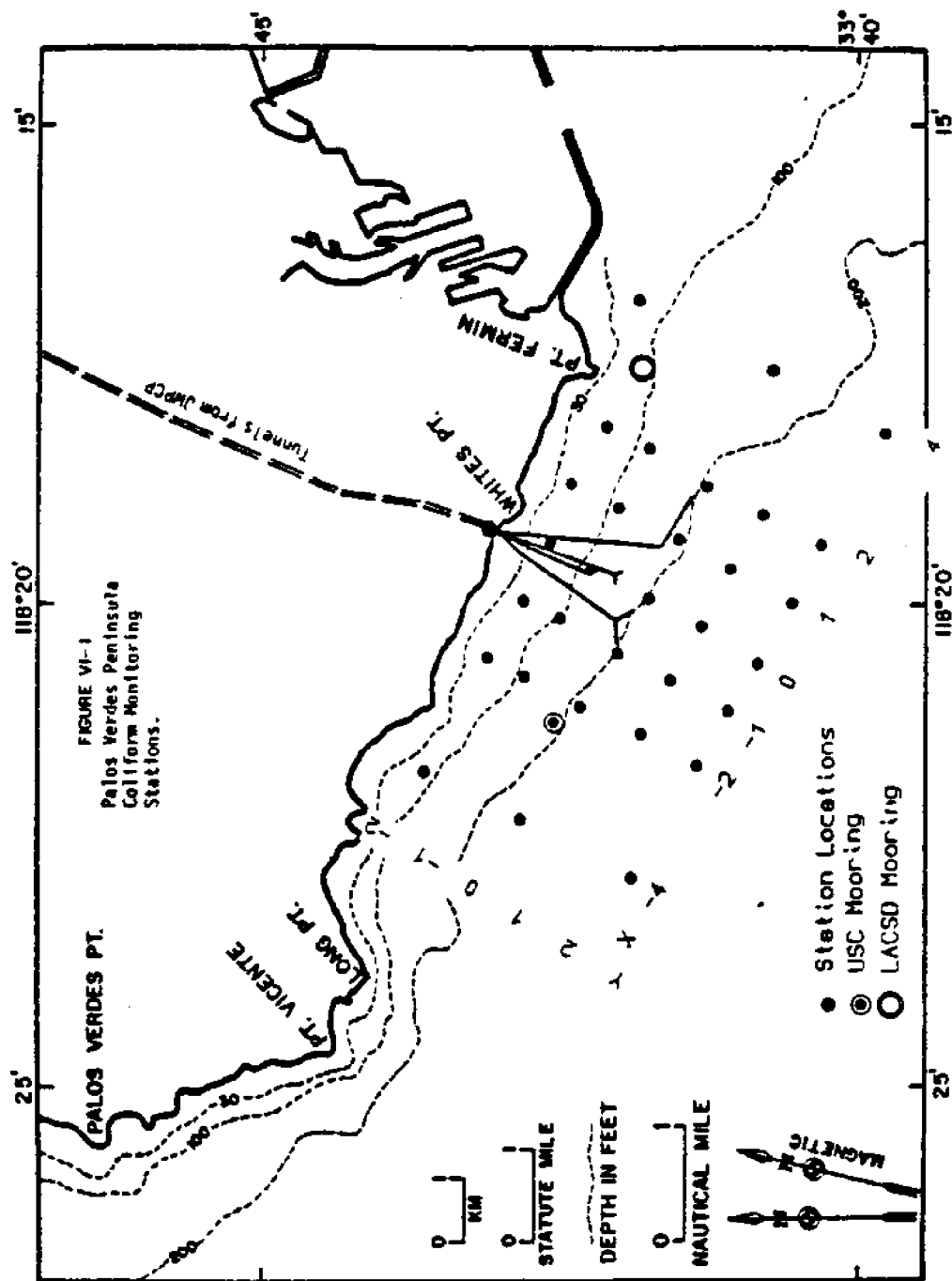


FIGURE 1.1 Map of the study region off the Palos Verdes peninsula showing the locations of the hydrographic grid stations, the USC mooring and the LACSD mooring. Also shown are the LACSD's outfalls.

reasons. First, the shelf where our mooring was located and where the LACSD outfalls lie is very narrow and slopes steeply compared to more typical continental shelves, (Pickard (1963) states that "average" gradients for continental shelves are 1 in 500, and that average shelf widths are 65 km). The slope of the shelf off Palos Verdes Peninsula is on the order of 1 in 100 and the shelf break lies only 2-3 km from the coastline. Second the Palos Verdes Peninsula protrudes into the Southern California Bight, an area of the California coast already recognized as having the most complex circulation patterns with respect to the large scale current systems identified in the region (Tsuchiya, 1980). Thus the sudden change of orientation of the coastline and the shelf at the peninsula, from a north-south to an almost east-west alongshelf orientation is an added complication. Third, the area is distinguished by the presence of Santa Monica Bay immediately to the north, the large shallow, breakwater enclosed harbor area of Long Beach to the south, and Santa Catalina Island located directly offshore at a distance of 22 miles.

This study describes significant aspects of seasonal, event and tidal time scale variability in the temperature field for the shelf region off the Palos Verdes Peninsula. Statistical analyses of the temperature data from this specific location include monthly seasonal statistics which are compared with the results of earlier studies. This statistical characterization of the local temperature structure near the LACSD outfalls is used to evaluate the role that natural processes play in the evolution of the effluent plume.

Historical data sets collected from two nearby California Cooperative Oceanic Fisheries Investigations (CalCOFI) survey grid locations, and from the pier at San Clemente (see figure 1.2 for locations) provide multiyear average seasonal patterns in temperature and salinity for direct comparison with the mooring records, and for estimates of the seasonal changes in the importance of temperature variability to the density stratification on the shelf. Climatic studies of the southern California area prepared by the Naval Oceanography Command Detachment also provide multiyear monthly averages of sea surface temperatures, winds, etc. A time series of wind for January to May, 1985 has been collected from a National Weather Service instrument located on the Platform Beta offshore oil platform located about 20 miles from the mooring site (see figure 1.2 for Platform Beta location).

One of the most important considerations to the far field dispersion and dilution of the effluent plume is the ambient density regime in the water column above the diffusers. Temperature and salinity both contribute to the density structure on the shelf off of Southern California. It has been observed that a large amount of the spectral energy in density and temperature variability on the southern California shelf is at near-tidal frequencies (List and Koh, 1976, Winant and Bratkovich, 1981, Bratkovich, 1985). This study statistically characterizes variability in temperature stratification levels on seasonal and event scales and evaluates how this variability affects the tidal signal in temperature and density.

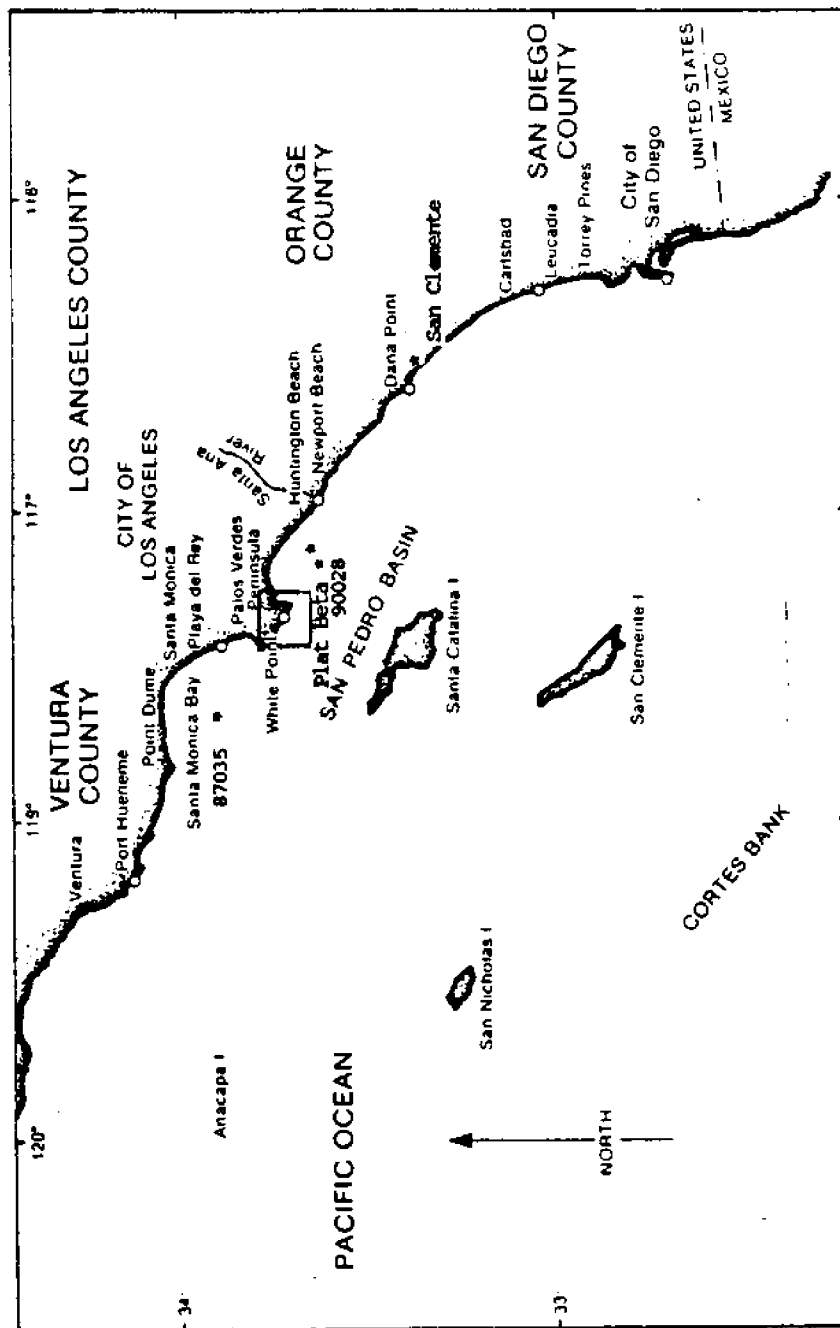


FIGURE 1.2 Map of the Southern California Bight showing the specific area of this study off the Palos Verdes Peninsula (see box). Locations of CalCOFI stations 90028, and 87035 are also shown as well as the San Clemente pier location from which ten years of monthly averaged temperature and salinity data are used. Platform Beta is the offshore oil platform from which wind data were collected at three hour intervals. (figure adapted from SOOWEP 1983-1984 biennial report).

The location of the study area was chosen to be near the sewage effluent outfalls. The LACSD treats approximately 365 million gallons of sewage effluent each day at its Joint Water Pollution Control Plant (JWPCP) in the city of Carson. All of this effluent receives primary treatment consisting of coarse filtering to remove grit and sand, addition of flocculants and settling to separate out solids and skim off floatables, and additional filtering by moving screens to remove grease and remaining suspended solids. At present some percentage of the effluent is given secondary treatment where bacteria and pure oxygen are added to the effluent to breakdown organics. Bacteria are then removed by a second addition of flocculants and further settling. The primary and secondary treated fractions of the effluent are mixed after treatment and are then pumped from the JWPCP plant to the diffuser system on the Palos Verdes shelf.

The effluent is discharged through the two newest and largest multiport diffusers extending out from Whites Point. Each of these diffusers is in about 60m of water 2.5km off the coast. The inside pipe diameters of these outfalls are 2.28 m and 3.04 m. Effluent exits the diffuser pipes through small (5 to 15 cm diameter) ports in the outfall pipes spaced at several meter increments along the last 1000m of the pipe. Discharge velocities at these ports are estimated to be about 3 m/s. The multiport diffuser system is designed to produce maximum initial dilutions of the effluent with the surrounding seawater. In the case of the LACSD outfalls off Whites Point initial dilutions are at least 1:100 or greater.

These high initial dilutions are achieved nearly immediately as the effluent exits from the discharge ports, however over the next few hours further mixing is estimated to produce only 5 to 10 times greater dilution. Near the ports, mixing is accomplished in buoyant jets, and governed by the momentum and buoyancy of the discharge, however after a period of several hours the diluted effluent plume tends to stabilize at a depth of comparable ambient density in the water column and is acted upon by coastal oceanographic processes. Since concentrations of various toxics contained in the effluent (particularly coliform bacteria) are generally still at unacceptably high levels, it is important to understand how these oceanographic processes will interact with and affect the effluent plume over periods of several hours to several days.

2.0 HISTORICAL BACKGROUND

Studies of the temperature and density fields on the continental shelf of the Pacific coast of North America have been made using a number of differing data sets and resolve a broad range of spatial and temporal scales. Liepper (1955) used a combination of sea surface temperatures, pier-end temperatures and hydrographic temperature data to study tidal frequency fluctuations which commonly manifest themselves as peaks in the energy spectra of temperature time series data. He identified internal waves with periods of about 12 hours at all the locations from which he had data, and measured vertical motions as great as 12 m. In addition, he explained erratic temperature variability which could not be explained by internal waves as the result of "cold spots" formed by horizontal variations in tidal frequency currents over an irregular bottom in the presence of stratified water layers. Bratkovich (1985) compared power spectra for temperature time series taken in winter and in summer at a cross-shelf array of moorings off Del Mar. The results showed that tidal frequency variability at 1, 2, 3 and 4 cycles per day are dominant features in the energy density spectra in all seasons, and temperature variability levels at tidal frequencies tend to be larger in summer relative to winter. Winant and Bratkovich (1981) used data from the same array of sensors to perform a seasonal study of current and temperature variability for one transect of the southern California shelf. In both of these studies, peaks in the energy spectra were clearly evident near 1 and 2 cpd and at the higher harmonic frequencies of the tide.

More detailed analyses of temperature variability at frequencies greater than 1 cpd have been considered for single day data sets. Howell and Brown (1985) identified a packet of 'solitons' on the shelf resulting from the interaction of shelf topography with a large amplitude internal wave. Their data set consisted of a 28 hour time series of current and temperature data from a single mooring located in 133 m on the continental shelf off northern California. Events were identified by increases in mid-depth temperatures with 1-3 hour durations associated with velocity oscillations in the cross-shelf direction which they were able to closely approximate with models of internal solitons in a two layer fluid.

Diurnal heating and cooling cycles in the ocean have been empirically studied and modelled. Stommel et al. (1969) did careful studies of single day heating events in an initially homogeneous body of water. Their study was made in an offshore oceanic environment known to be relatively constant over large horizontal scales, and for these reasons radiative heat flux and vertical mixing could be assumed to be the dominant processes. Results of the analysis of nine diurnal cycles recorded show considerable variability in day to day heating and in the depth of thermocline established over the course of the day in the relatively homogeneous mixed layer which formed during the night. Dickey and Simpson (1982) modelled diurnal sea surface temperatures and heat storage in the upper ocean. Driving functions in their models are atmospheric fluxes of heat and momentum (e.g., solar insolation and time varying wind stresses). They summarized

observations of diurnal sea surface temperatures from a variety of locations, with ranges of the diurnal temperature reported between 0.1 and 1.7 °C. Four separate studies made between 33 and 35° N latitude (the latitude at which the data for this study were collected) have a much smaller diurnal range of temperatures (between 0.1 and 0.3 °C). Liepper (1955) recognized diurnal cycles in temperature time series collected off the coast of Southern California. He isolated these cycles by averaging monthly temperatures for each 2-hour period of the day.

Probably the most extensive area of temperature related work on the shelf involves longer term data sets and is aimed towards describing seasonal averages and observed variations between seasons. Huyer (1977) documents such seasonal features on the shelf off Oregon using a set of intermittent moored temperature measurements which span a nine year time interval. She defines a representative 'winter' and 'summer' month distinguished from one another by temperature stratification and by T/S plots used to identify water types. She concludes that on the Oregon shelf seasonal hydrographic variability is due to geostrophic currents which flow southward in summer and northward in winter, and to seasonal variation in the wind field which leads to enhanced upwelling during the summer and produces a summer water mass of low temperature and salinity water on T/S plots. California Cooperative Oceanic Fisheries Investigation (CalCOFI) data also provide large scale pictures of changes in the coastal temperature, salinity and density fields as well as averaged cross-

sections for the different seasons (CalCOFI Atlas #25, and #30, 1982). Cairns and Nelson (1970) approach the problem of describing seasonal variation in a slightly different manner, producing plots of vertical thermal gradients and their changes with depth and with season. They used hourly temperature data collected from nine thermistors on an oceanographic tower located in 18 m water depth on the shelf near San Diego. Analysis of more than a year of data showed an increase in monthly temperature variance from 0.2 (degrees C²) in January to 5.6 (degrees C²) in May and August. Cairns and Nelson also observed that semidiurnal temperature variations believed to be of tidal origin were present throughout the year.

Coherence of the density field in the alongshelf and cross-shelf direction has also been studied from at least two perspectives. List and Koh (1976) and Winant (1983), although starting with quite different types of data, approached the alongshelf temperature coherence problem in similar fashion. In each case they defined high, intermediate, and low frequency bands of variations, and then characterized the spatial variability in these separate bands using covariance and cross correlation techniques. Winant, using a 60 km array of moorings located along the 30 m isobath off San Diego, concluded that low frequency variability is more coherent over a given separation than higher frequency variability. List and Koh, using 5 years of daily temperature records from 18 stations along the Pacific coast, support this conclusion, observing almost no coherence of high frequency variability between stations only a few miles apart.

Statistical analyses of the temperature and salinity data collected on the shelf off Palos Verdes during 1985 from both moored instruments and hydrographic ship surveys have provided monthly seasonal statistics which are compared with results of the studies cited above.

Tsuchiya (1980) has described the circulation off southern California as being more complex than anywhere else in the California Current system. On the large scale the California Current flows southeastward past Point Conception where it is deflected offshore and away from the coast. To the east, inshore of the California Current, is a northwest flow identified as the Southern California Countercurrent. Tsuchiya (1980) describes this as the inshore rim of a large cyclonic eddy that extends from Point Conception southward to 31 to 33° N. Hickey (1979) describes flow in the southern California Bight in terms of the Southern California Eddy. She connects the eddy with an eastward bend of the California Current near 32° N. When the mainstream of the current reaches the coast some of the water turns northward forming the Southern California Countercurrent. This pattern is further complicated by the possibility of southward flow inshore of this northward flow, particularly in the southern half of the bight between January and May, but also in the northern half during April. This is believed to reflect a seasonal onshore-offshore shift in the positions of the California Current and Southern California Countercurrent. During the months October to January the California Current moves offshore and the countercurrent intensifies, but from

April to May the California Current swings inshore and often eliminates the countercurrent.

Mean geostrophic currents computed from dynamic height anomalies are given for each month in the Climatic Study of the Southern California Operating Area (1983). These show currents of 1.5 cm/s towards 348° (true) in January within a 1° by 1° square centred over Santa Catalina island and the Palos Verdes Peninsula. In February, March and April the average monthly current swings to about 30° and has a velocity of 0.5 cm/s. In May the current velocities begin to increase and the direction of the current swings back towards the north (0°). This trend continues until December which has the largest current velocities of 2.6 cm/s towards 350° .

3.0 DATA BASE

The field measurement component for the Sea Grant/LACSD project was initiated in January of 1985. Figure 3.1 is a time line showing the distribution and extent of the numerous sub-studies which were carried out in the study area during 1985. Two distinct sampling methods were used, with the intent of resolving a broad range of both spatial and temporal scales of variability during the winter season. The first was a mooring deployed for four months to collect current and temperature data from four sensor sets located at depths of 12, 23, 34, and 45 m and anchored to the bottom in 55 m of water, (see figure 3.2). The second component of the measurement program was a series of hydrographic surveys. These surveys, each of which took approximately 12 hours to complete, were made on 7 separate days during the last 2 weeks of January 1985. They were all carried out between 9 a.m. and 9 p.m., and individual surveys were separated by between 36 to 72 hours. Each survey cruise made vertical profiles of temperature, fluorescence and percent light transmission from the surface to 80 m maximum depths at 25-35 locations within the 4 km (cross-shelf) by 8 km (alongshelf) grid (centered over the LACSD's 2 major diffusers off White's Point, see figure 1.1). On each cruise a more extensive set of data parameters, including measurements of conductivity, ammonia, nitrate, nitrite, phosphate, silicate, chlorophyll-a and phaeopigment was sampled using a water-pumping profiling package at nine of the central stations located nearest to the outfall diffusers.

1985 FIELD MEASUREMENTS

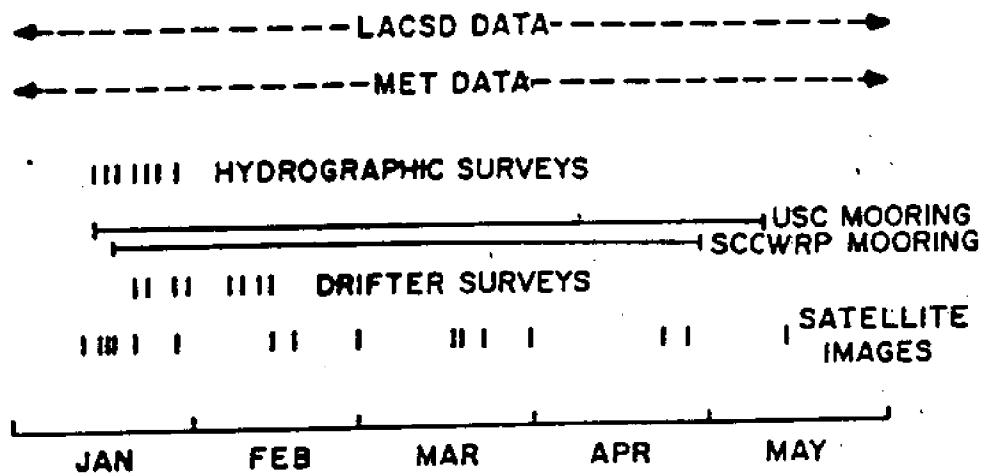


FIGURE 3.1 Time line of the 1985 field observations made as part of the study entitled "Physical and Chemical Oceanographic Variability in the region near the Los Angeles County White's Point Outfall. This study examines the USC mooring data which span the period from January 14 to May 9. Data from the hydrographic surveys, and drifter surveys as well as LACSD buoy data, NWS meteorological data and satellite imagery is also utilized.

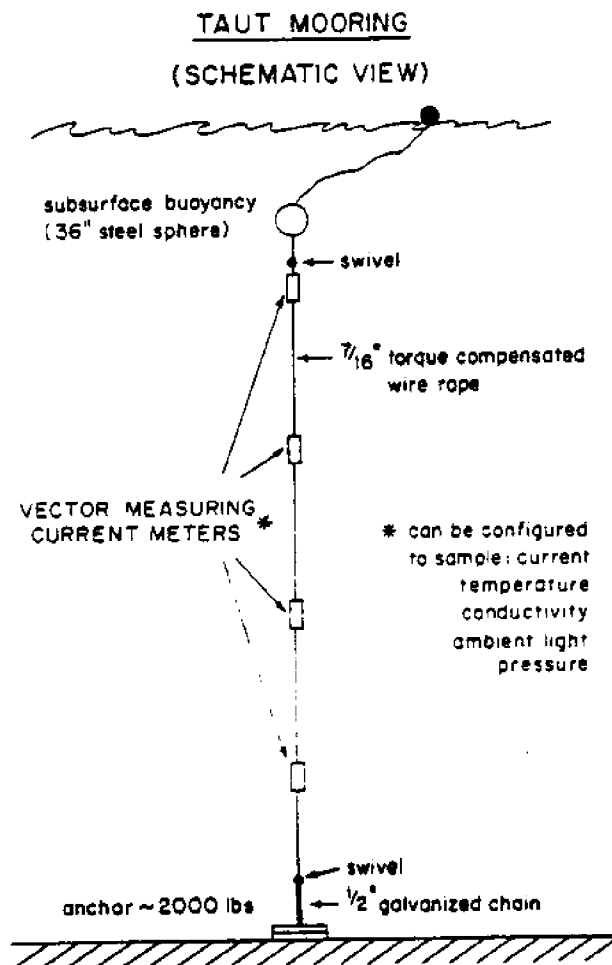


FIGURE 3.2 Schematic of the USC mooring deployed at the location shown in figure 1.1. The mooring included VCM's at 12, 23, 34, and 45 meters depth and was anchored in 55 meters total water depth.

Hydrographic data, collected by Dr. Burton Jones, have already undergone calibration and preliminary data processing, and have been assembled into standard format on a computer system. Temperature data are tabulated at depth intervals of approximately 4 m from the surface down to maximum depths of 80 m for the offshore stations. Additional temperature and salinity data from the hydrographic cruises include measurements made during vertical pumping profiles (usually resulting in one averaged temperature/salinity value per 10 m) and near surface temperature and salinity lines made while the ship was running parallel to the coastline from one end of the grid to the other (approximately one temperature/salinity value per 100 m of horizontal displacement).

The mooring data provide a continuous four month time series of temperature values at two discrete depths (see figure 3.2). Temperature circuit failure caused the thermistor data recorded at two of the four instruments to be unusable, however the temperature time series from the sensors at 12 and 34 m are usable for the purposes of this study and have been averaged to hourly values in order to have them in a standardized form.

As part of the Sea Grant / LACSD project 40 to 50 IR satellite images were collected by Dr. Gary Kleppel at the Scripps Satellite Oceanography Facility during the four month intensive field measurement period. Figure 3.1 shows the dates for which exceptionally clear images are available. Wind data at 3 hr intervals were collected from three nearby locations and from the anemometer attached to the

data collection buoy maintained by the LACSD (located in 25 m of water just off Point Fermin). The LACSD has also provided the other data which is collected from this buoy, including the temperature data from ten thermistors which extend into the water column below the mooring. Monthly statistics generated from the hourly temperature time series at the LACSD buoy's top and bottom sensors (located at 4 and 19 m depth) are compared with similar statistics for the USC mooring.

Several additional data sources exist for support and comparison with the above sets. CalCOFI temperature and salinity data from the nearby stations 87035 and 90028 (see figure 1.2 for the location of these two stations) have been obtained from the CalCOFI data base. This data base spans a 20 year period (1950-1970) during which hydrographic sampling was done on an irregular schedule. As a result, data are available for each month for anywhere from 0 to 8 years out of the 20 years. Pier-end data (gathered by the National Oceanic and Atmospheric Administration) such as that used by List and Koh, (1976) have been derived from Robinson (1972), for a ten year period at San Clemente. This data set contains an almost continuous record of daily temperature and salinity measurements. Monthly averages of this data were compiled for each month over the ten years. These multiyear averages of the seasonal pattern in temperature and salinity on the southern California continental shelf near Palos Verdes provide a useful baseline for comparison of the seasonal pattern in the January to May record from the USC mooring. Additionally they allow for some

rough estimates of density contributions from temperature and from salinity.

4.0 ANALYSIS

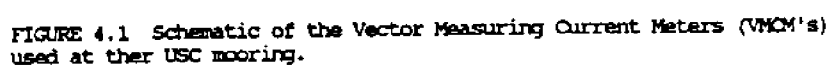
TEMPERATURE DATA COLLECTION AND REDUCTION

The temperature sensors of the EG&G VMCM's (figure 4.1) used at the USC mooring incorporate the 1.5 inch thick aluminum alloy cover of the watertight instrument casing as a probe. Mechanically this is achieved by placing the very small spherical thermistor into a hole drilled into the center of a bolt which is then screwed into the underside of the cover plate. The response time ($1/e$ folding time) of this thermal mass has been determined to be approximately four minutes. The instrument sampling procedure used for the January 14 to May 9, 1985 deployment was to record onto magnetic cassette tape four minute averaged values of two current components and temperature.

Temperature and current measurements were averaged to hourly values using a one hour long running mean filter with data quality checks made at each four minute average. At the same time, these data values were translated from hexadecimal code into units of degrees Centigrade for the temperature, and for the current components into units of centimeters per second.

HYDROGRAPHIC TEMPERATURE DATA COLLECTION AND REDUCTION

During the seven January hydrographic cruises vertical profiles were made between the surface and maximum depths of 80 m. The individual profiles are located using the X and Y grid coordinates for the hydrographic grid shown in figure 1.1. Two distinct instrument packages were used to make the profiles, the first, a vertically



profiled package which was used at every station, collected depth, temperature, fluorescence and transmissometer data from instruments connected to an onboard computer by cable. The second, which required more time to operate, was used only at nine of the central stations. This instrument consisted of a submersible pump which returned water to an onboard autoanalyzer that measured ammonia, phosphate, silicate, nitrate and nitrite. Additionally, water from this pumping system was passed through temperature and conductivity sensors, and samples were collected and used for chlorophyll-a and phaeopigment measurements.

The data from the vertically profiled package were averaged from one second averages to 10 second averages which provided measurements separated by 4 m at the maximum rates of descent through the water column. Data from the pumping package were separated into discrete samples at 10 m depth increments. After calibration and filtering, data for all variables were transferred to a specially designed data base system.

On five of the hydrographic cruises (January 16, 18, 23, 25, and 28), vertical temperature profiles (using the vertically profiled package) were made at the grid location -2,0 which is only 250-300 meters distant from the mooring location. Also, on three of these days (January 23, 25, and 28) vertical pumping package profiles using a different temperature sensor were also made at this station. The IACSD vessel which was used to make drifter drogue studies of surface currents in the area used its BT instrument to produce four vertical temperature profiles immediately next to the mooring (Jan. 23, 28, 30

and Feb 11). Altogether 12 vertical temperature profiles are available to intercompare with the moored temperature sensors.

Time series temperature values at the mooring were linearly interpolated from the nearest hourly value on either side of the time at which the hydrographic casts were made. Comparison of these fixed depth temperature points from the mooring with the vertical temperature profiles produced from these casts gives the following results, (figure 4.2). Agreement is good (less than 0.2°C difference) for the vertical profiles made on January 23 and 28. On January 25, the 12 m value shows good agreement with the vertical profile but the 34 m sensor value on this day is 0.5°C too high. Vertical temperature profiles made on January 16 and 18 were extremely "noisy" and are not shown. Pumping profiler vertical temperature profiles show good agreement on January 25 and 28, but on January 23 the pumping profiler values are almost 2.0°C higher than temperatures at the mooring. Although rough estimates of the horizontal temperature gradients have been made (see below) from the hydrographic data, it is difficult to know how much affect the horizontal gradients have on the results in figure 4.2. Two points which can be made are, one; maximum observed horizontal temperature gradients were less than $0.5^{\circ}\text{C}/\text{km}$, and while gradients of this size could explain differences of up to 0.2°C between mooring and hydrographic profiling data, gradients would have had to have been more than an order of magnitude larger than this to explain the 2.0°C differences seen on January 23. Two; comparison of vertical temperature profiles made by the two distinct instrument

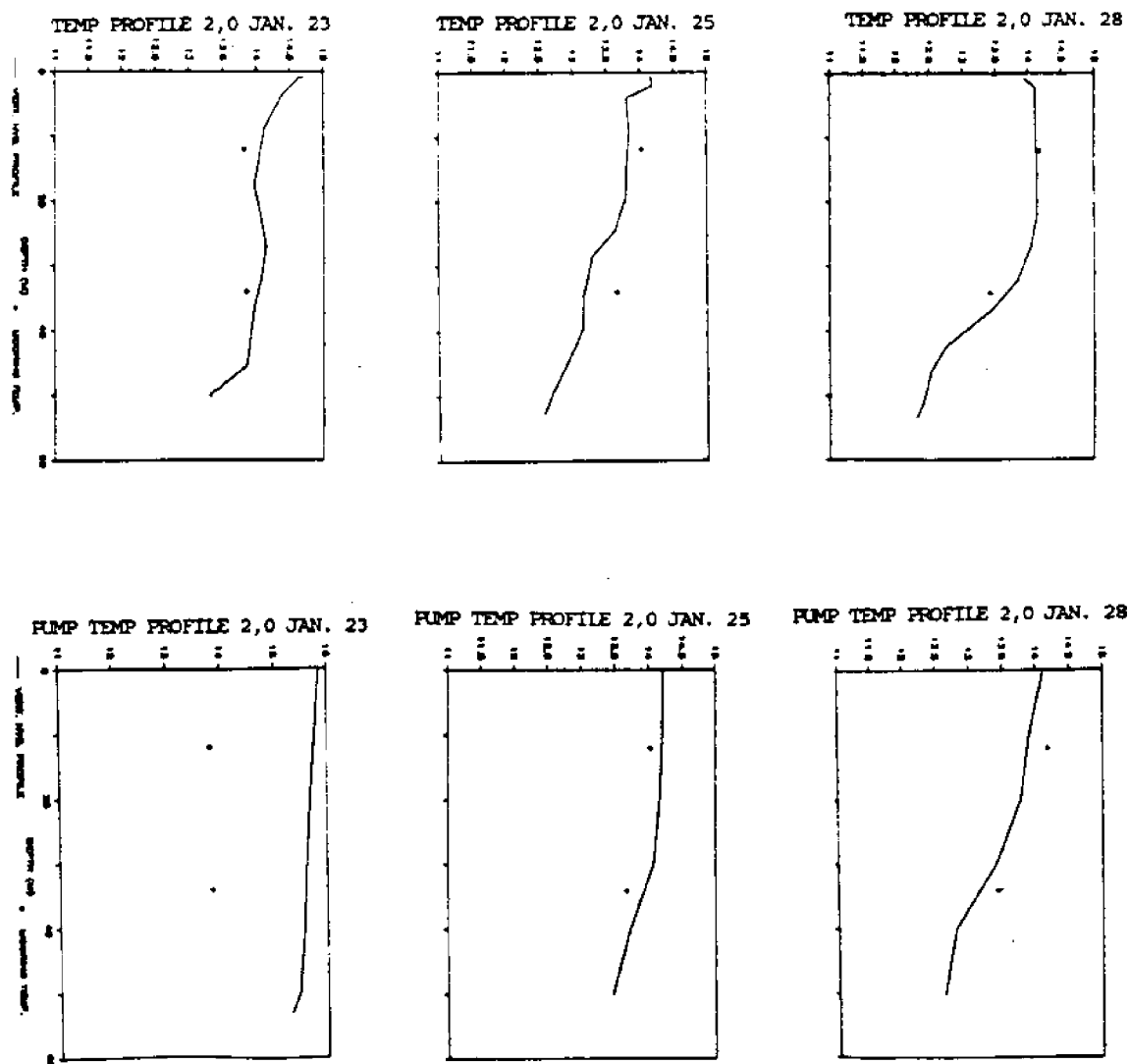


FIGURE 4.2 Vertical temperature profiles made at the nearest hydrographic grid station to the mooring location on the indicated days during January 1985. The grid coordinates are -2, 0 and can be found on figure 1.1. This hydrographic grid station was 250 m from the USC mooring. Points at 12 and 34 m depth are the interpolated temperatures from the VMOM records.

packages at the same time show inconsistencies with the idea of a horizontal gradient offset, (i.e. on January 25 pump temperature profiles are higher than mooring values, while vertical profiler temperatures are lower, and on January 28 the opposite situation exists).

INTERCALIBRATION PROCEDURE AND RESULTS

It was decided that because horizontal temperature gradients were not known, only the four BT profiles made on January 23, 28, 30, and February 11, directly adjacent to the mooring, should be used to calibrate the temperature time series. A least squares fitting routine taken from Bendat and Piersol (1971) was used to determine a linear correction to apply to the time series data based on the BT values. This calibration was limited by (1) the small number of BT casts, (2) the fact that the BT data are clumped near the beginning of the mooring deployment period, (3) the limited range of temperatures observed in the period when the BT profiles were made relative to the range of temperatures seen in the full four month time series and (4) the accuracy and resolution of the IACSD BT instrument (the IACSD BT data had a resolution of 0.1°C , the accuracy is believed to be approximately 0.1°C also).

TABLE 4.1, COMPARISON OF LACSD BT TEMPERATURE DATA WITH 12 AND 34 M VMCM TEMPERATURE DATA

	Jan. 23		Jan. 28		Jan. 30		Feb. 11	
	BT	VMCM	BT	VMCM	BT	VMCM	BT	VMCM
Depth								
0.0 m	14.4		14.6		14.3		13.7	
12 m	14.3	13.85	14.5	14.18	14.2	14.02	13.6	13.28
25 m	14.2		14.0		14.2		13.2	
34 m	13.9	13.67	13.9	13.66	13.8	13.78	12.4	12.36
47 m	13.1		12.6		12.9		11.7	

Results of the least squares fitting indicate that at the 95% confidence level the temperatures from the moored thermistors are within ± 0.1 to 0.3°C of the BT temperatures, this difference varies somewhat with the particular temperature value.

Prior to the 1986 deployment, the VMCM's were tested in a water bath. Since the instruments were set up to record in the range from $5 - 17^{\circ}\text{C}$ the water bath was cooled to approximately 15°C . Results of the five hour test show maximum differences between the thermistors which were located at 12 and 34 m on the mooring of 0.05°C . Comparison of the thermistor recorded temperatures with thermometer readings made in the water bath indicate that absolute temperatures were correct to $\pm 0.05^{\circ}\text{C}$. These water bath results, which were made after the temperature time series had already been corrected to the BT results and extensively analyzed, suggest that the absolute accuracy of the thermistor data can be improved once a high accuracy calibration regime has been implemented for the instrumentation.

GENERAL THEORY OF TEMPERATURE VARIABILITY

In a fluid such as seawater, heat is transferred by four distinct mechanisms, 1) conduction, 2) advection, 3) turbulent diffusion and 4) radiation. Conduction is a molecular level process and in the upper ocean advection, turbulent diffusion and solar insolation are usually much more important mechanisms of heat transfer.

A general equation to describe the variability in temperature at a point in the ocean may be written as follows:

$$\frac{\partial T}{\partial t} + u \cdot \nabla T = K \nabla^2 T + S$$

This equation may be rewritten following Reynolds decomposition and assuming constant eddy diffusion;

$$\underbrace{\frac{\partial T}{\partial t}}_{(a)} + \underbrace{u \frac{\partial T}{\partial x} + v \frac{\partial T}{\partial y} + w \frac{\partial T}{\partial z}}_{(b)} = \underbrace{K_x \frac{\partial^2 T}{\partial x^2} + K_y \frac{\partial^2 T}{\partial y^2} + K_z \frac{\partial^2 T}{\partial z^2}}_{(c)} + \underbrace{\frac{1}{\rho C_p} \frac{\partial I}{\partial z}}_{(d)} + \underbrace{K \nabla^2 T}_{(e)}$$

Section (a) of equation (2) represents the local change of temperature with time at a fixed point. (b) is the advective component of temperature change due to the advection of the gradient field by the horizontal and vertical components of velocity. Section (c) includes diffusive effects on the temperature variability due to turbulence, and other physical processes parameterized by the Reynolds decomposition. Section (d) represents solar insolation. Section (e) is the temperature change due to molecular diffusion processes and is

assumed to be negligible for the purpose of this study. K_x and K_y are horizontal eddy diffusivities, K_z is the vertical eddy diffusivity, and K is the molecular diffusivity.

Although the data collected during this study were not intended to be used in any kind of rigorous closure of the above equation, some rough estimates of the relative importance of the different components associated with various physical processes occurring over a limited range of temporal and spatial scales can be made using simple scaling analysis.

Estimates of all terms in the above equation were made for four 65 hour periods which are centered on January 18, 23, 25, and 28. These are the dates of the four complete hydrographic cruises made while the VMCM's were operating. On these days estimates of cross-shelf and alongshelf temperature gradients can be made which are synoptic in time with current and temperature records from the mooring.

Temperature cross-sections from the hydrographic cruises made on January 18, 23, 25 and 28 provide finite difference estimates of the temperature gradient over survey lines running parallel to the coast and perpendicular to the coast. Temperature data collected at the hydrographic stations lying on the line $X=0$ and on the line $Y=0$ (see figure 1.1 for locations of these lines in the survey grid) were interpolated linearly to determine exact values at 10 m depth. Absolute values of the differences in these 10 m temperature values between adjacent stations (each separated by 1 km on the hydrographic survey lines $X=0$, and $Y=0$) were averaged to give a single absolute

horizontal temperature gradient value for each of the four days in both the alongshelf and cross-shelf directions. When net differences over the five kilometer line of stations were used instead of the 1 km differences the horizontal gradient components are about a factor of three smaller, indicating that significant variability in the horizontal temperature gradient components occurs at length scales of between 1 and 5 km (assuming simultaneity of measurements). These same hydrographic measurements are also used to determine values for the horizontal spatial scales appropriate to the terms in (c).

Scale values for the cross-shelf and alongshelf velocity components (u , v) were calculated by averaging a 65 hour series of hourly data (already subjected to low pass filtering, using a 65 hour triangle weighted filter, to remove diurnal and higher frequency variability). These averages were centered on the middle of the hydrographic cruise days. Identically low pass filtered time series of the temperature at 12 m and the temperature gradient between 12 and 34 m were used to obtain the difference in temperature with time, and the average vertical temperature gradient over the same 65 hour period. An estimate of the diffusive term can be obtained using the vertical temperature gradient.

Dividing the change in temperature over each 65 hour period by the average vertical temperature gradient for the same time interval gives an estimate of the magnitude of the vertical velocity component;

$$w = \frac{\partial T / \partial t}{\partial T / \partial z}$$

This value calculated for w , which may be interpreted as the mean vertical 'upwelling' velocity, is a maximum value assuming that all temperature variability is due to vertical movement of the local vertical component of the temperature gradient. The expected values of w are immeasurably small, far less than the resolution threshold of modern current measuring instrumentation. One of the important source terms for temperature variation can be estimated using the formula;

$$H = \frac{1}{\rho C_p} \frac{\partial I}{\partial z} \quad \frac{\partial I}{\partial z} = -k I_0 e^{-kz}$$

Where long term averaged solar insolation values for January are 100 Watts/m², Nelson and Husby (1983). density of water is set at 1.025 gm/cm³, and C_p is 1 cal/cm³. Using the formula in Smith and Baker (1978) one can obtain an optical attenuation depth according to;

$$K_t^{-1} = 8.78 - 7.51 \cdot \log C_k$$

where C_k is the average chlorophyll concentration in the water down to one attenuation length (estimates of C_k were made from averaged cross-shelf sections of the chlorophyll concentrations made during the hydrographic cruises, value used was 0.7 ug/l). The inverse of the attenuation length K_t is gamma (k). Using this formula an optical attenuation depth of 10 m was calculated. Actual values may be influenced by light absorption by effluent material, etc. which this computation did not consider.

Pond and Pickard (1983) state that eddy diffusivities are approximately equal to eddy viscosities (usually within an order of magnitude). They give values of horizontal eddy viscosities (A_h) between 10^{-5} - 10^{-1} m^2/s and vertical eddy viscosities A_z between 10^{-5} - 10^{-1} m^2/s . In computations to estimate the contribution of turbulent motions and smaller scale advective fluxes (parameterized as diffusive terms) to the variability, maximum values of the diffusivities were used.

Estimates of each of the terms for each of the four cruise days are shown in table 4.2 below. Most terms are comparable in size to the local rate of change, (dT/dt) , however horizontal advective terms appear to play a dominant role. Since eddy diffusion terms were computed using maximum diffusivity values they may actually be a few orders of magnitude smaller.

For all but very small scales the diffusive terms (e) are negligible because of the relatively small values of molecular diffusivity of water. Carslaw and Jaeger (1959) give a molecular diffusivity value for water, $K = 0.00144$ cm^2/sec .

TEMPERATURE VARIABILITY SCALES

Band pass filtering (using moving triangle weighted filters of 65 hour and 360 hour length) was done on the 12 and 34 m temperature time series to separate seasonal, event and tidal scale variability (figures 4.3 and 4.4). Preliminary inspection of the high and low frequency components of variability extracted in this way shows

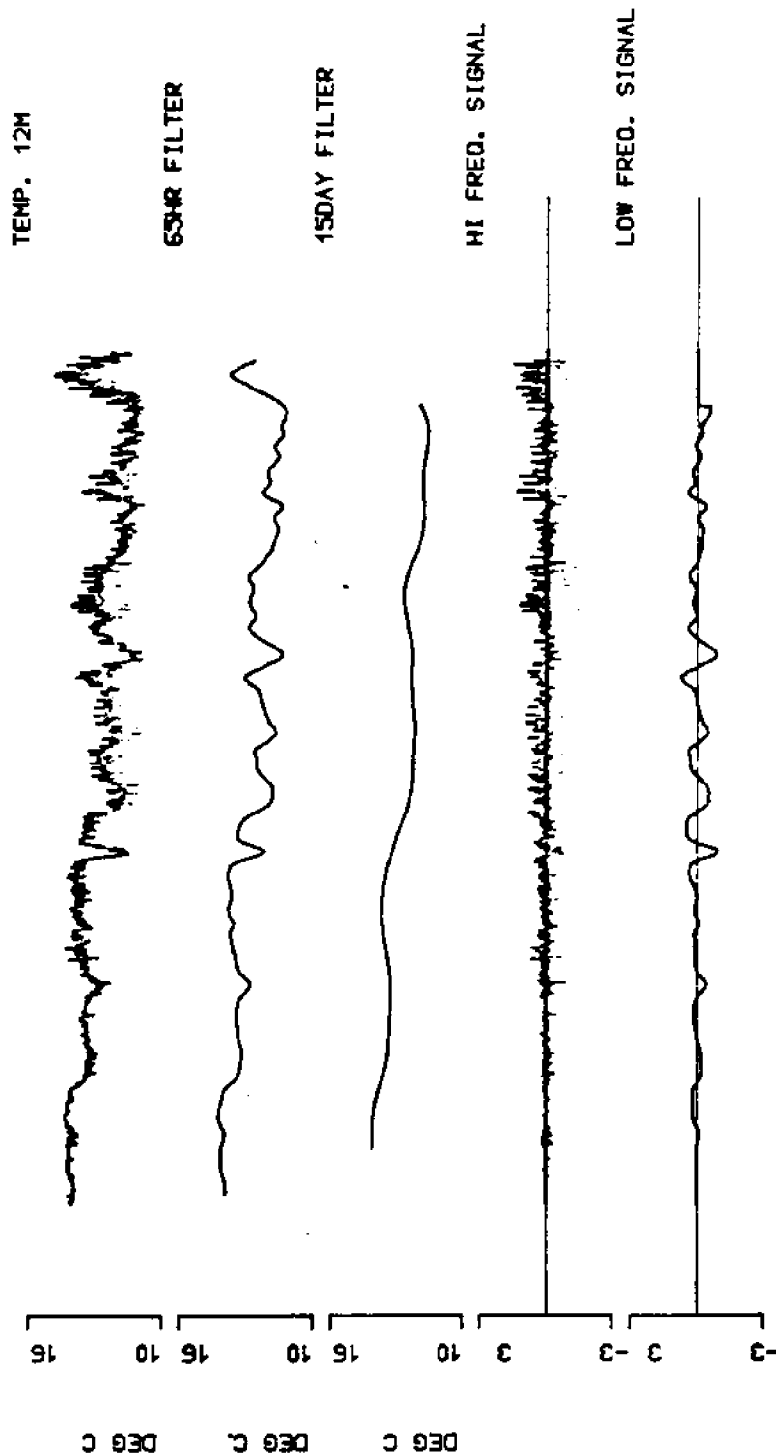
TABLE OF RELATIVE ESTIMATES FOR TERMS IN HEAT BUDGET EQUATION
FOR JANUARY 18, 23, 25, AND 28 ON THE PALOS VERDES SHELF

Day	$\frac{\partial T}{\partial t} + u \frac{\partial T}{\partial x} + v \frac{\partial T}{\partial y} + w \frac{\partial T}{\partial z} = K_x \frac{\partial^2 T}{\partial x^2} + K_y \frac{\partial^2 T}{\partial y^2} + K_z \frac{\partial^2 T}{\partial z^2} + \frac{1}{\rho C_p} \frac{\partial I}{\partial z} + K \nabla^2 T$									
18	0.8	4.0	20.0	1.0	0.7	5.0	0.01	0.7	---	---
23	0.5	0.5	3.0	0.4	1.0	2.0	0.002	0.7	---	---
25	1.0	2.0	0.1	2.0	1.0	0.8	0.008	0.7	---	---
28	0.9	1.0	20.0	0.7	0.9	2.0	0.009	0.7	---	---

(all values are times 10^6 , units are $^{\circ}\text{C}/\text{sec}$)

TABLE 4.2 Results of scaling analysis of terms in heat budget for four 65 hour periods in January on the shelf off the Palos Verdes peninsula. Scaled values for the various terms in the equation above were calculated from mooring and hydrographic data centered in time on the four hydrographic cruises made on January 18, 23, 25 and 28. See text for description of the various terms in the equation above, and for the methods used to calculate, or estimate the different terms.

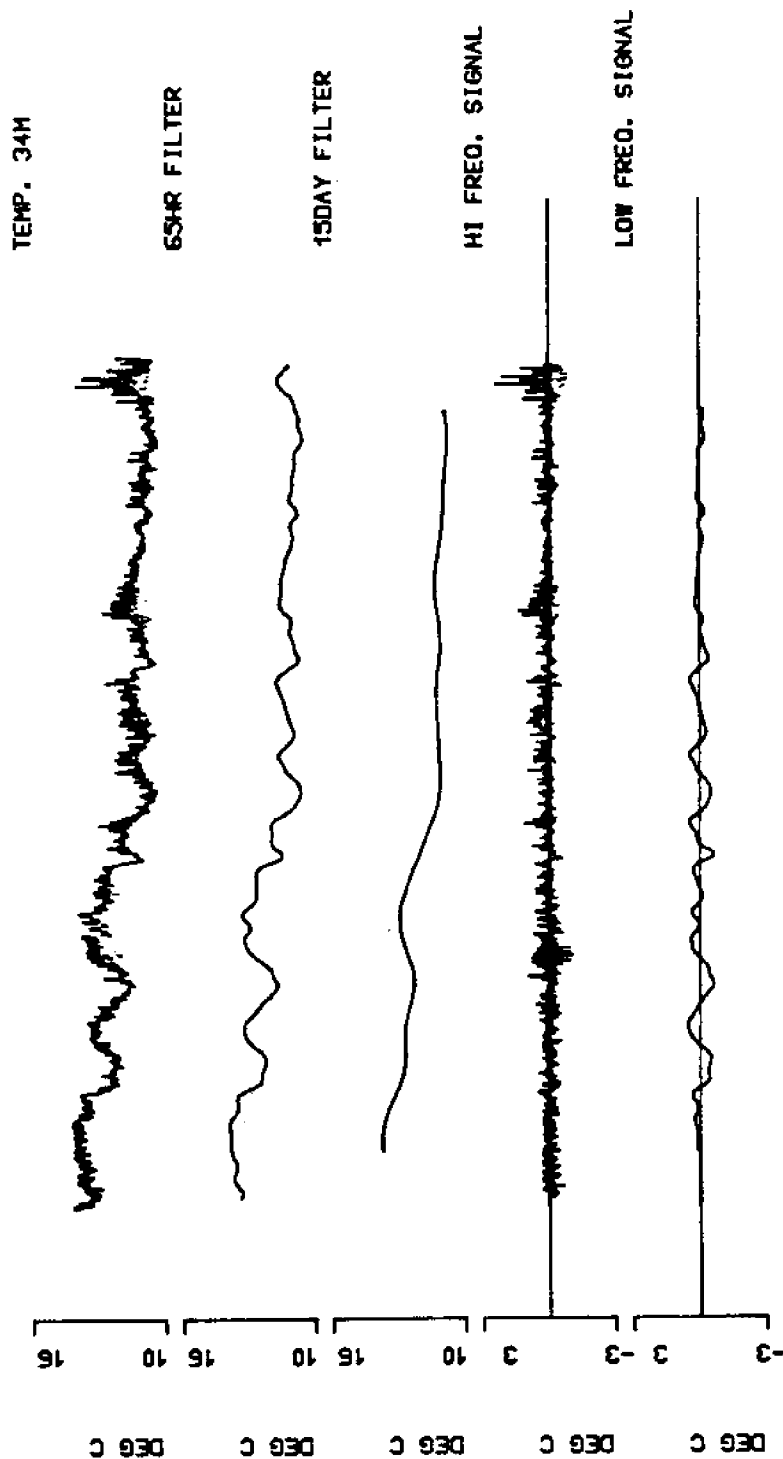
TEMPERATURE DATA AT 12M DEPTH USC MOORING



DECIMAL JULIAN DAYS (0-150)

FIGURE 4.3 Selectively filtered temperature data over the entire deployment period from the 12 meter temperature sensor. Top plot is unfiltered data, second is filtered to remove tidal and diurnal variability, third is filtered to remove individual events. The high frequency signal is raw data minus 65hr filtered data, and the low frequency signal is the 65hr filtered data minus the 15 day filtered data.

TEMPERATURE DATA AT 34M DEPTH USC MOORING



DECIMAL JULIAN DAYS (0-150)

FIGURE 4.4 Selectively filtered temperature data over the entire deployment period from the 34 meter temperature sensor. Top plot is unfiltered data, second is filtered to remove tidal and diurnal variability, third is filtered to remove individual events. The high frequency signal is raw data minus 65hr filtered data, and the low frequency signal is the 65hr filtered data minus the 15 day filtered data.

comparable standard deviation of temperatures at diurnal and shorter time scales as at event scales of several day duration (Table 4.3). The monthly standard deviations in table 4.3 also show the rapidly increasing ratio of high to low frequency variability as the year progresses. The magnitude of the high frequency variability increases with time at both the 12 and 34 m depths as can be seen in plots of the high frequency signal for January-May, and in the monthly standard deviations for the high frequency signal in table 4.3. The low frequency variability appears to peak in February and March and then to decrease.

Power spectra of the temperature and current time series data (figure 4.5) show clear peaks at frequencies of 1, 2 and 4 cycles per day. These spectra were calculated from limited portions (10 day segments) of the time series records from the moored instruments and resultant spectra were then averaged to produce the spectra in figure 4.5, as a result low frequency bands (less than 0.1 cpd) are not estimated. Frequency resolution of these power spectral density plots are not sufficient to allow an inertial period (about 22 hours for this latitude) peak to be distinguished from the diurnal peak. Examination of progressive vector diagrams of current data showed no obvious clockwise rotation that would indicate inertial motions.

Autocorrelation function estimates of the 12 and 34 m temperature records made for each month of the deployment (figure 4.6) show a clear increase in the strength of the diurnal and semidiurnal signal as the year progresses. In January the 12 hour peak in the

Table of Statistics for the 12 and 34 Meter Temperatures and the Temperature Gradient

12 m Temperature:

Mo.	Hrly. Sig.		65Hr filter		15day filter		Hifreq Sig	Lofreq Sig
	Mean	St.Dev.	Mean	St.Dev.	Mean	St.Dev.	St.Dev.	St.Dev.
Jan.	14.06	0.125	—	—	—	—	0.069	0.103
Feb.	13.41	0.313	13.41	0.241	13.43	0.150	0.177	0.160
Mar.	12.41	0.757	12.42	0.607	12.46	0.387	0.369	0.426
Apr.	12.04	0.676	12.03	0.512	12.02	0.371	0.408	0.217
May.	12.60	1.323	—	—	—	—	0.609	0.204
Avg.	12.80	0.975	—	—	—	—	0.343	0.272

34 m Temperature:

Mo.	Hrly. Sig.		65Hr filter		15day filter		Hifreq Sig	Lofreq Sig
	Mean	St.Dev.	Mean	St.Dev.	Mean	St.Dev.	St.Dev.	St.Dev.
Jan.	13.66	0.289	—	—	—	—	0.180	0.107
Feb.	12.63	0.556	12.63	0.455	12.66	0.198	0.279	0.335
Mar.	11.37	0.614	11.36	0.504	11.39	0.371	0.294	0.298
Apr.	11.03	0.384	11.03	0.273	11.04	0.196	0.253	0.119
May.	11.31	1.222	—	—	—	—	0.588	0.047
Avg.	11.90	1.100	—	—	—	—	0.300	0.242

Temperature Gradient:

Mo.	Hrly. Sig.		65Hr filter		15day filter		Hifreq Sig	Lofreq Sig
	Mean	St.Dev.	Mean	St.Dev.	Mean	St.Dev.	St.Dev.	St.Dev.
Jan.	0.018	0.012	—	—	—	—	0.008	0.004
Feb.	0.036	0.021	0.035	0.015	0.035	0.006	0.013	0.010
Mar.	0.048	0.026	0.048	0.009	0.049	0.004	0.023	0.008
Apr.	0.046	0.031	0.046	0.015	0.045	0.009	0.026	0.008
May.	0.053	0.077	—	—	—	—	0.047	0.006
Avg.	0.040	0.033	—	—	—	—	0.023	0.008

Temperature units = degrees Centigrade
Temperature gradient units = degrees Centigrade/meter

TABLE 4.1 Statistics for the time series of temperatures from the USC mooring. Includes monthly means and standard deviations and the overall means and standard deviations for the unfiltered signal at 12 and 34 m depth and for the temperature gradient calculated between these depths. Also for the 65 hour filtered signal, the 15 day filtered signal, and the low (65 hour filtered data minus 15 day filtered data) and high (unfiltered data minus 65 hour filtered data) frequency components of the signal. Blanks identify means and standard deviations not included because filter cutoff reduced the number of usable data points. See figures 4.3, 4.4, and 4.8 for time series plots of these data sets.

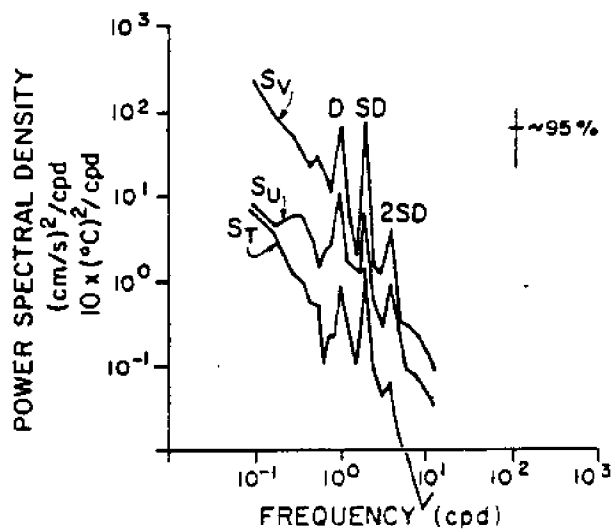


FIGURE 4.5 Power spectra (S_u = cross-shelf, S_v = along-shelf, S_t = temperature) for the current components and temperature from the 12 meter instrument. All three show distinct peaks at diurnal, semi-diurnal, and twice semi-diurnal frequencies. (A. Bratkovich, unpublished data).

JANUARY FEBRUARY MARCH APRIL MAY

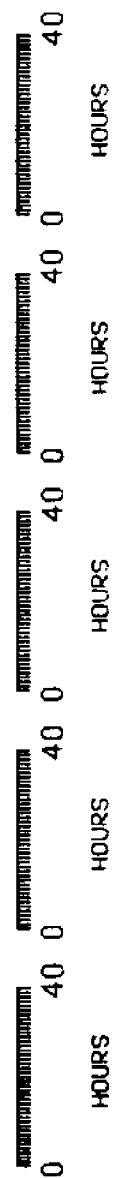
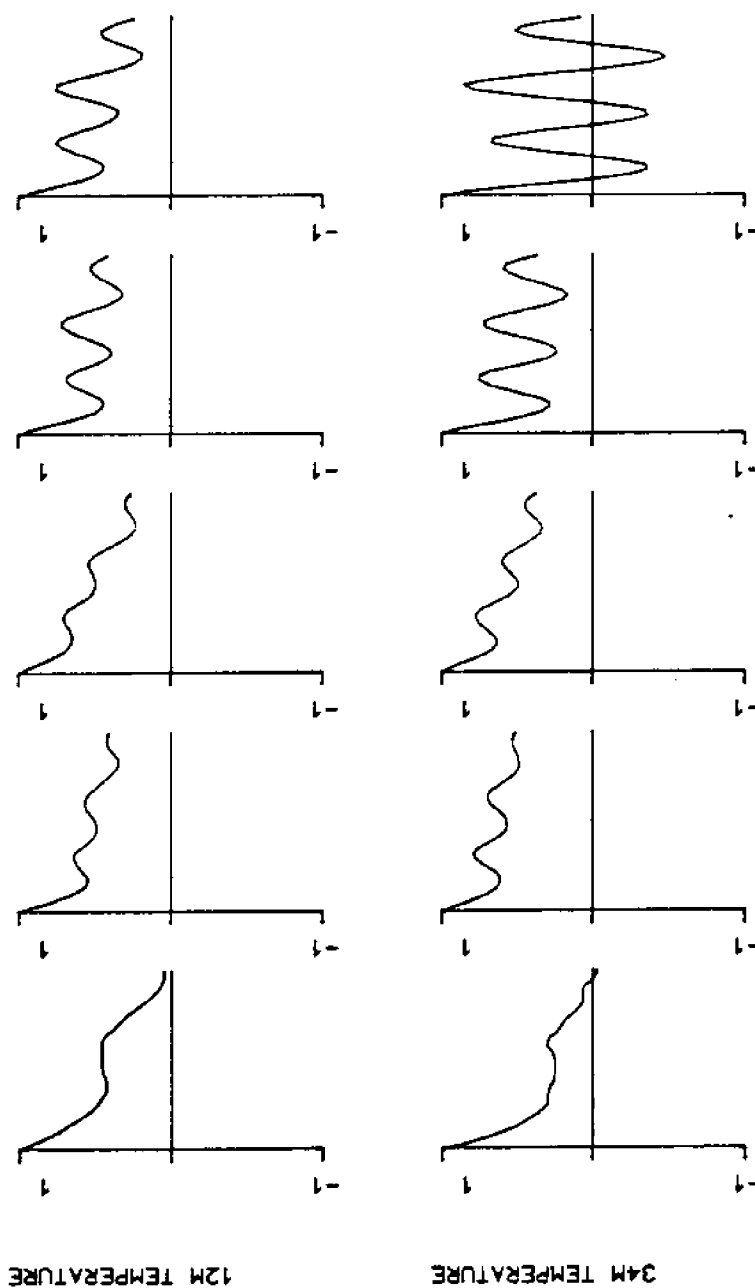


FIGURE 4.6 Autocorrelations of the temperature time series from the 12 and 34 meter sensors for each month of the deployment period.

autocorrelation is absent and only the 24 hour, diurnal, peak remains. There is a steady trend of increasing amplitude of the variability in the autocorrelation values occurring at semidiurnal and diurnal time scales between January and May.

The 15 day filtered temperature signal from both the 12m and 34m instruments shows a trend of gradually decreasing temperature (-0.02 $^{\circ}\text{C}/\text{day}$) between January and April, and then an increase in temperature ($+0.03$ $^{\circ}\text{C}/\text{day}$) at both depths in the early part of May. These results can also be seen in the monthly statistics in table 4.3. In the first 4 months of 1985 temperatures dropped by 2.5 $^{\circ}\text{C}$ at 34 m depth, and by 2 $^{\circ}\text{C}$ at 12 m. Then in the first part of May the averaged temperatures at both depths began to rise, going up by about 0.3 $^{\circ}\text{C}$ at both depths.

TEMPERATURE PROBABILITY DENSITY DISTRIBUTIONS

Probability density plots of temperature for each month (figure 4.7) show again the trend of decreasing temperatures from January to March at both 12 and 34 m. The probability density distribution of the vertical temperature stratification in degrees C per meter when compared between months indicates that there is a gradual increase in levels of stratification over the January - May period (from an average value of 0.018 $^{\circ}\text{C}/\text{m}$ in January to an average value of 0.053 $^{\circ}\text{C}/\text{m}$ in May, see table 4.3) even though temperatures at both 12 and 34 m depths are decreasing. Figure 4.8 shows the full four month time series of the temperature gradient as well as band pass filtered data. The high frequency signal varies over a considerably greater range of

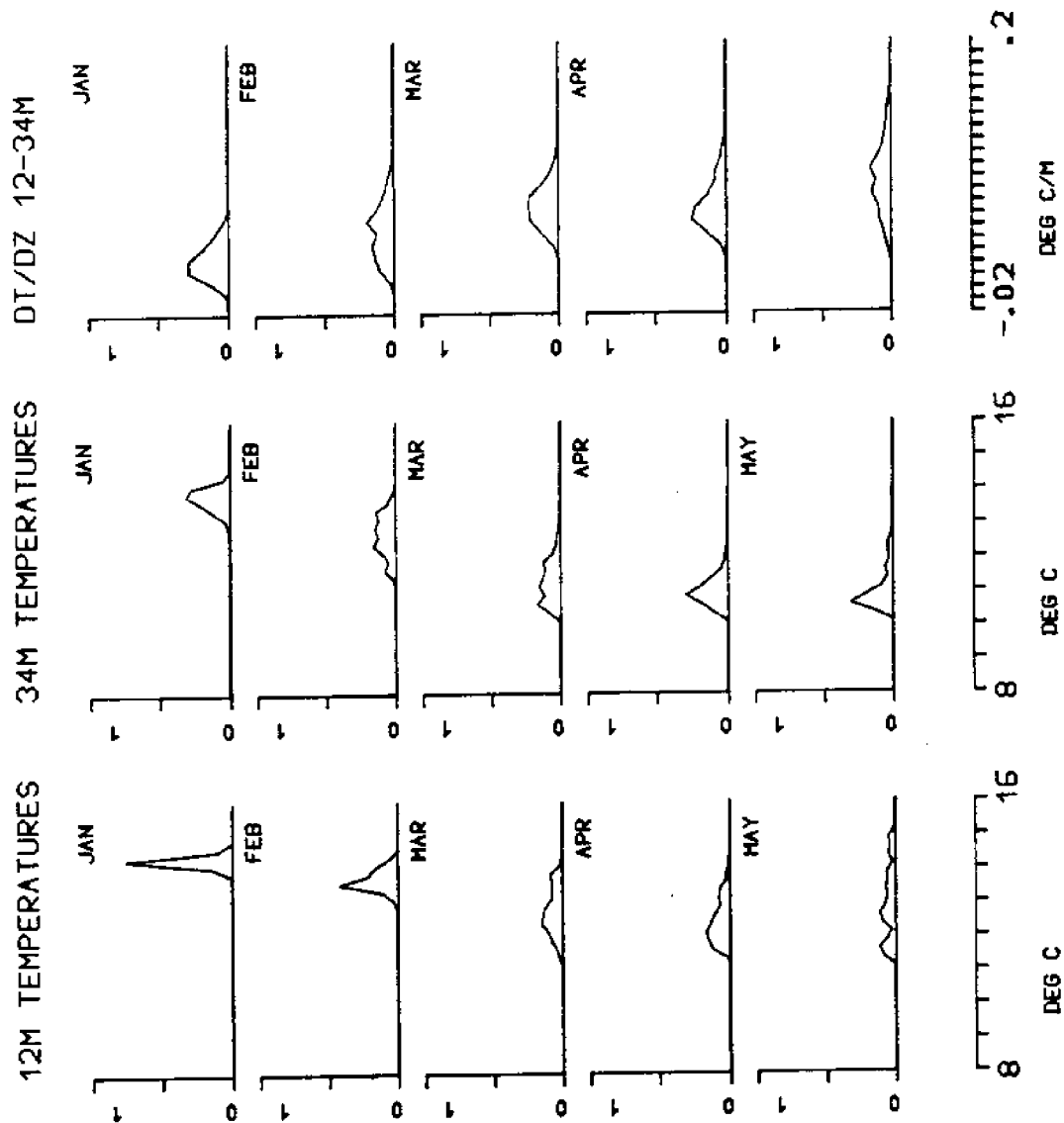
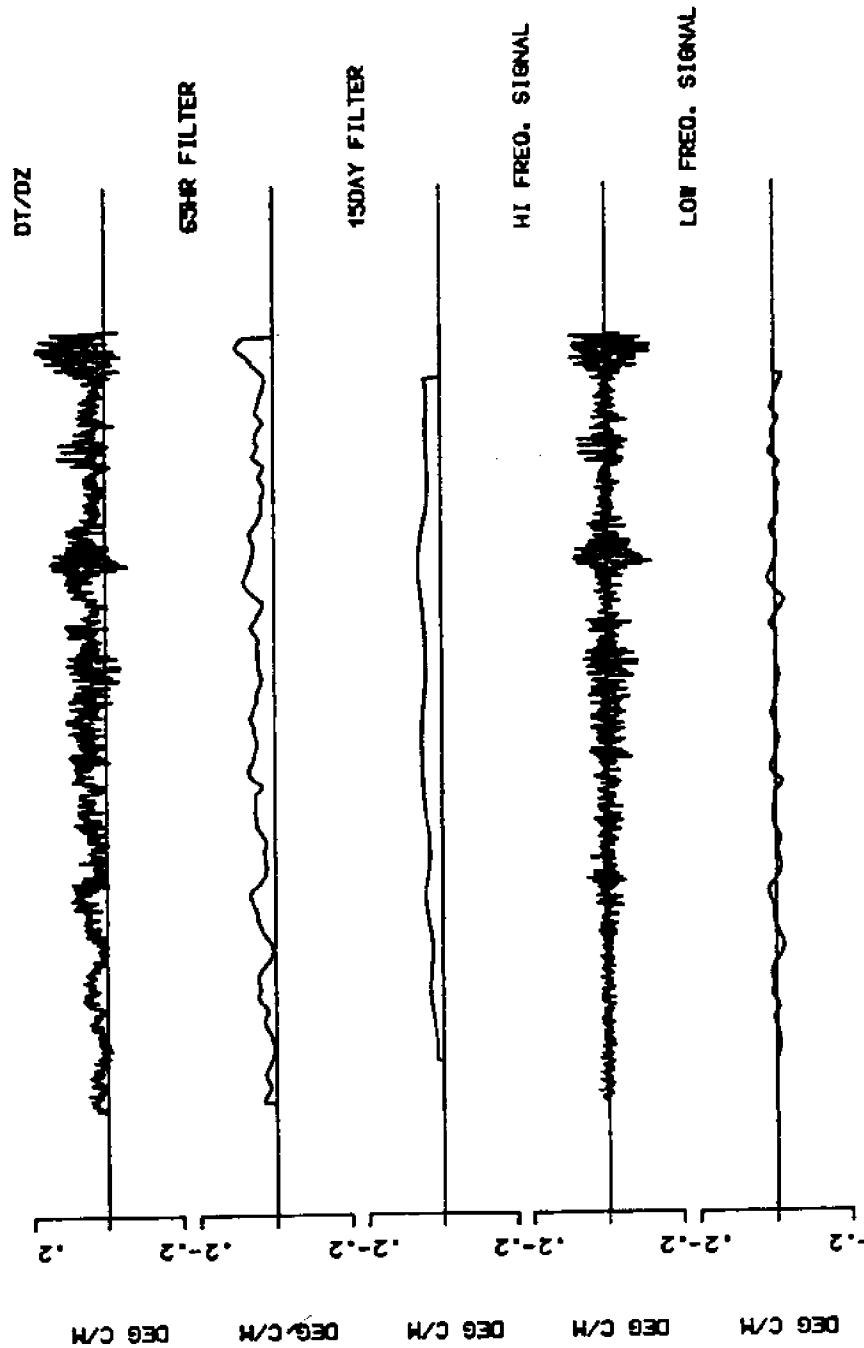


FIGURE 4.7 Probability density plots of the 12 and 34 meter temperatures, and the temperature gradient between the 12 and 34 meter sensors for each month of the deployment period.

DT/OZ BETWEEN 12M AND 34M DEPTH USC MOORING



DECIMAL JULIAN DAYS (10-150)

FIGURE 4.8 Selectively filtered temperature gradient data over the entire deployment period between the 12 and 34 meter temperature sensors. Top plot is unfiltered data, second is filtered to remove tidal and diurnal variability, third is filtered to remove individual events. The high frequency signal is raw data minus 65hr filtered data, and the low frequency signal is the 65hr filtered data minus the 15 day filtered data.

values than does the low frequency signal (standard deviations for the high frequency signal are three times those for the low frequency signal). The probability density plots also show a gradual broadening of the temperature range and the development in March of a skewed distribution towards higher temperatures. Similar distributions are repeated in probability density plots of temperature stratification and imply the formation of warmer surface layers for brief periods.

AVERAGED DAILY CYCLES OF TEMPERATURE

In order to identify relationships between different variable fields collected in this study which have persistent daily features, 24 hour average daily cycles were assembled by averaging each hour of the day for the entire length of the time series. Isolating daily variability is also helpful when considering interactions with the effluent plume since discharge rates vary depending on time of day. One of the important monitoring programs of the LACSD is daily sampling of coliform bacteria concentrations in shoreline water samples collected each morning at seven points on the Palos Verdes Peninsula. If significant daily cycles in winds, currents and temperature stratification exist then they may produce a cycle in the coliform concentrations which varies with time of day.

Daily means were subtracted from each 24 hour period in order to detrend the data, and this results in the cycles being essentially demeaned. Thus in some cases, such as when there was an average monthly current that was other than zero, this must be taken into

consideration when examining the averaged daily cycle.

The diurnal temperature cycle for the temperature record at 34 m (figure 4.9) averaged over the entire 113 day time series shows an apparently semidiurnal cycle of heating and cooling with average temperature peaks at 3 a.m. and 3 p.m. and minimums at 9 a.m. and 10 p.m. The 3 p.m. maximum is stronger than that at 3 a.m. Figure 4.10 shows the averaged 24 hour cycle of temperature at 12 m. At 12 m the daily variation in temperature is similar to that at 34 m, with the most obvious difference being the flattening of the 3 a.m. peak and the 9 a.m. minimum. Dickey and Simpson (1983) observe that maximum net heating at the surface leads the maximum sea surface temperature by two to four hours. Assuming a 12 noon maximum in net heating at the surface for our study area the lead time is three hours.

These plots suggest that semidiurnal variability is more distinct at depth and becomes masked in the near surface region, probably due to a more diurnal solar-driven heating and cooling mode in the mixed layer. Attempts to fit these cycles to a sine-cosine wave equation of period 24 hours and 12 hours confirm this (Table 4.2). At 12 m the better fit was made with a 24 hour period wave with an amplitude calculated to be 0.1066 ± 0.0152 °C. The 34 m data was fit better by a 12 hour (semidiurnal) period wave and had an amplitude calculated as 0.116 ± 0.002 °C. This semidiurnal period variability is believed to be caused by internal tidal waves. It is probably intensified below the mixed layer where vertical density stratification is greater.

The average 24 hour cycle for the vertical temperature gradient

AVG'D 24HR CYCLE OF 34M TEMPERATURE

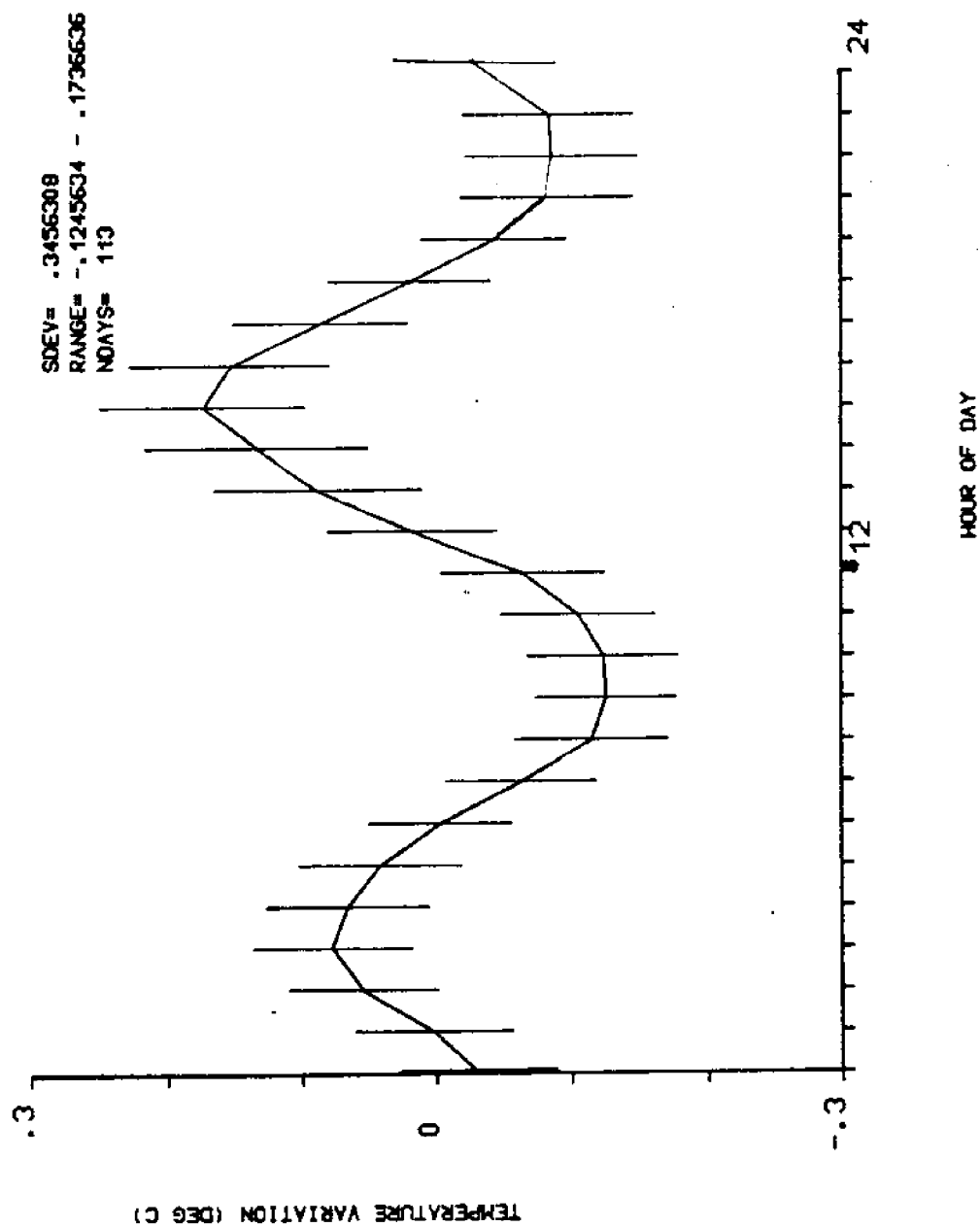
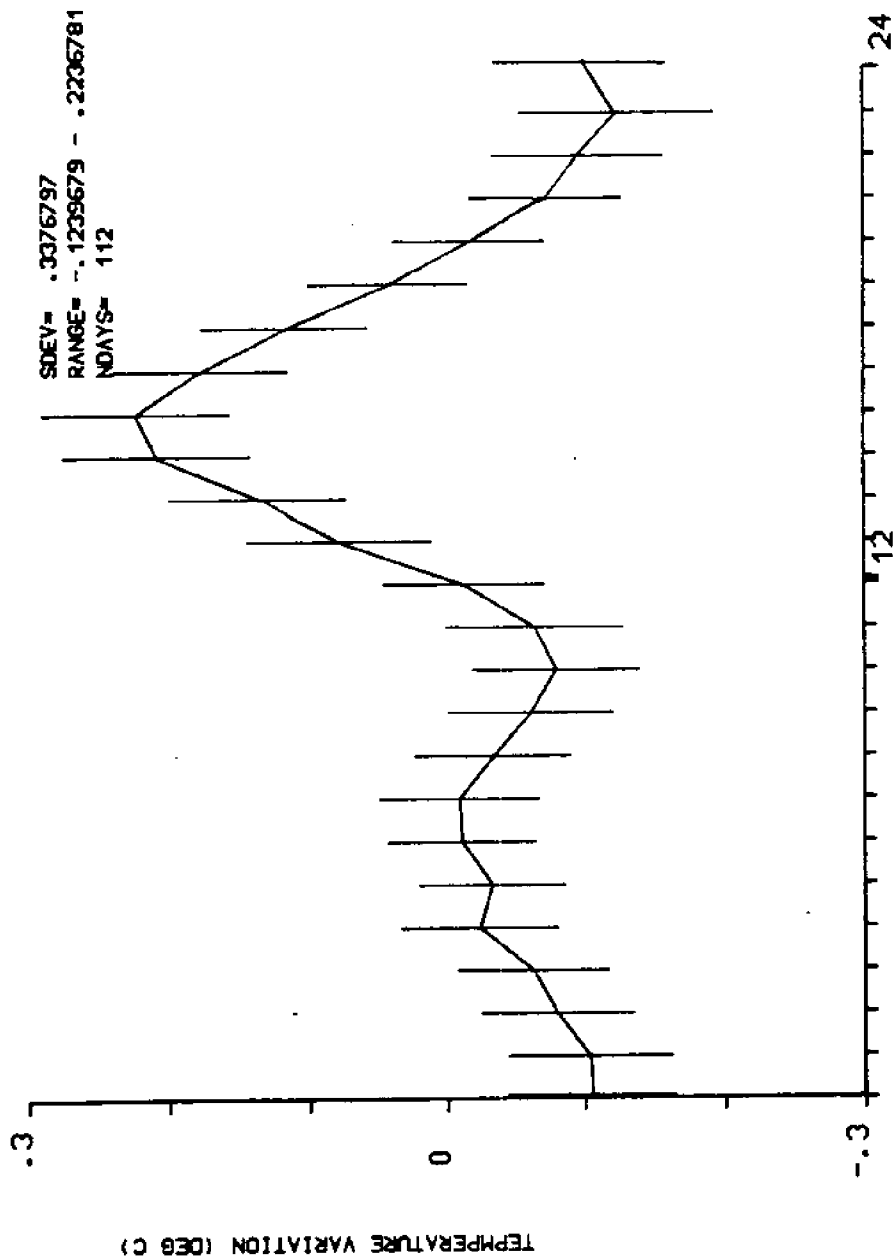


FIGURE 4.9 Averaged cycle of temperature variation at the 34 meter sensor over a 24 hour day. Produced by averaging all temperatures from similar times of day over the 113 day deployment period.

AVG'D 24 HR CYCLE OF 12M TEMPERATURE



HOUR OF DAY

FIGURE 4.10 Averaged cycle of temperature variation at the 12 meter sensor over a 24 hour day. Produced by averaging all temperatures from similar times of day over the 113 day deployment period.

Table of 24 and 12 Hour Sine-Cosine Wave Fit to Daily Averaged Cycles

File	24 hour				12 hour				Range	
	R**2	Ampl.	Phs.	StErr	R**2	Ampl.	Phs.	StErr	Min.	Max.
12m Temp.	0.75	0.106	2.9	0.015	0.63	0.091	-2.6	0.008	-0.12	0.22
34m Temp.	0.36	0.045	-4.3	0.02	0.92	0.116	-1.5	0.002	-0.12	0.17
Temp grad	0.86	0.004	4.4	.0002	0.43	0.002	2.0	.0004	-.006	.004
12m CS cur	0.87	0.828	4.7	0.097	0.46	0.439	-1.4	0.115	-1.12	1.30
23m CS cur	0.94	0.999	-5.1	0.081	0.27	0.288	-5.6	0.183	-1.40	1.03
34m CS cur	0.42	0.344	-3.9	0.067	0.88	0.723	4.6	0.098	-1.22	1.05
45m CS cur	0.22	0.286	3.8	0.085	0.97	1.240	4.0	0.083	-1.50	1.27
12m AS cur	0.94	2.189	-5.2	0.137	0.31	0.717	-4.7	0.446	-1.90	2.95
23m AS cur	0.95	2.157	-5.3	0.087	0.26	0.580	4.5	0.460	-2.05	3.16
34m AS cur	0.94	2.020	-5.3	0.125	0.32	0.697	5.1	0.440	-1.98	3.11
45m AS cur	0.94	2.040	5.4	0.123	0.31	0.671	3.8	0.450	-1.67	3.13
PB AS wind	0.97	1.630	0.8	0.065	0.24	0.395	-2.7	0.002	-2.00	1.34
PB CS wind	0.90	0.547	-1.3	0.045	0.44	0.268	-5.9	0.064	-0.80	0.59

Temperature and temp. grad. units=deg. C, current units=cm/s, wind units=m/s
Phase lags are in hours

TABLE 4.2 Results of sine-cosine wave fitting to the averaged daily cycles for the temperature, temperature gradient, current and wind data discussed in the text. Each averaged cycle was fitted with a 24 hour and a 12 hour period wave. R**2 values estimate the quality of the fit and the standard error gives an estimate of the accuracy of the amplitude. Range minimum and maximum values are taken from the averaged cycles before fitting. Only the 34 m temperature and the 34 and 45 m currents seem to be fit better by the 12 hour period sine-cosine wave which approximates semidiurnal variability.

(figure 4.11) shows a minimum at 3 a.m. local time. This can be predicted from an examination of the 12 and 34 m 24 hour cycles of temperature. At 34 m there is a temperature maximum at 3 a.m., but this early morning temperature peak is shifted and flattened in the 12 m data and the net result is a reduction in the temperature gradient at this period in the early morning. Table 4.4 shows that the averaged daily cycle of the temperature gradient was best fit by a 24 hour sine-cosine wave with an amplitude calculated as 0.004 ± 0.0002 °C/m.

CURRENT FIELD DATA

The VMCM instruments record current velocities from two sets of fans whose axes are perpendicular to each other. As they are sensed the two velocity components are automatically rotated to a north-south and east-west orientation by the VMCM, which has an internal magnetic compass. The northward and eastward velocity components are continuously averaged and in this particular case recorded to cassette tape every four minutes. In order to isolate the alongshelf and cross-shelf variability in the currents, the averaged, hourly north-south and east-west components were recombined and rotated 70 degrees counter-clockwise from magnetic north. This correction was chosen because it most closely aligned the alongshelf currents with the isobaths on the Palos Verdes shelf where the mooring was located. In the averaged cycles presented below, a positive value in the alongshelf direction represents a current moving alongshelf towards

AVG'D 24 HR CYCLE OF DT/DZ 12-34M

SDEV= 1.34774
 RANGE= -.6410834 - .3753709
 NDAYS= 112

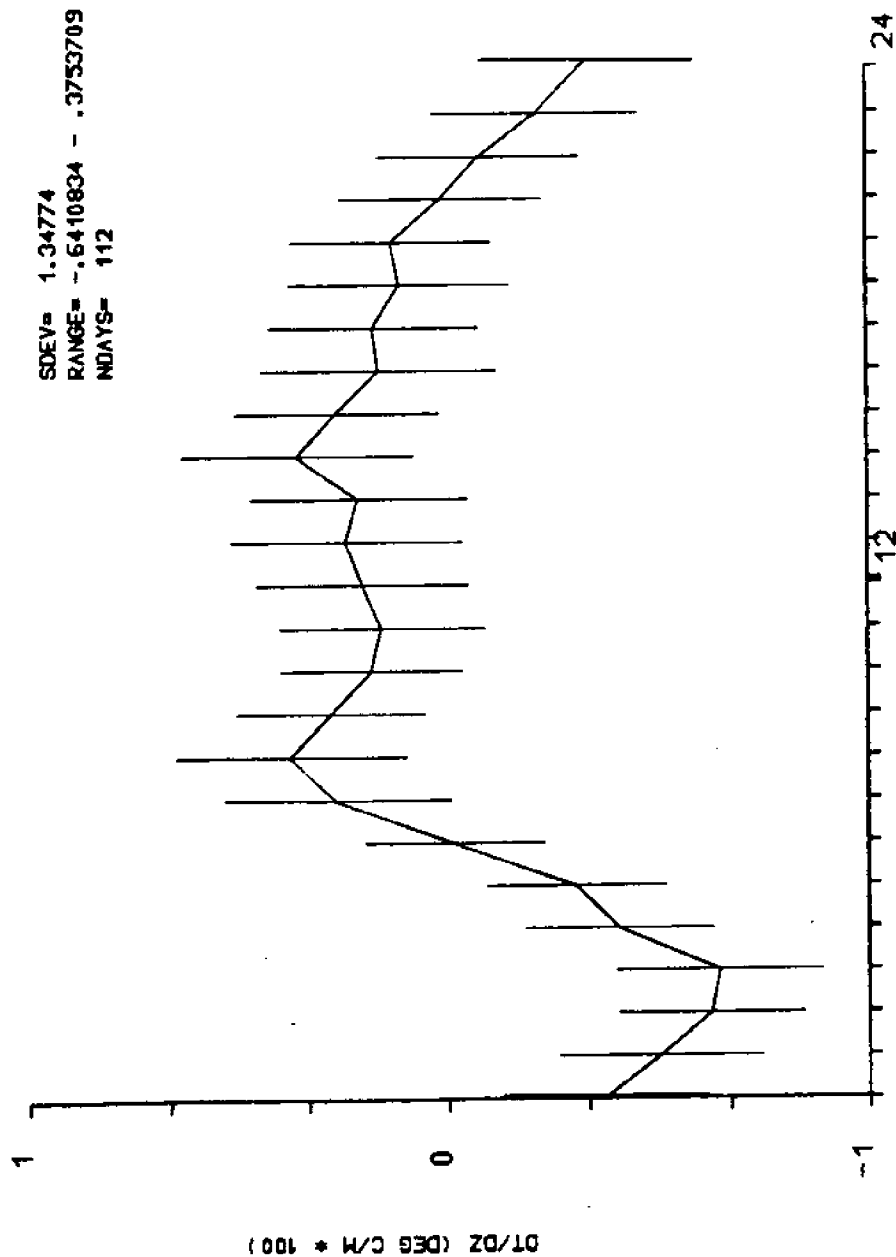


FIGURE 4.11 Averaged cycle of temperature gradient variation between the 12 and the 34 meter sensors over a 24 hour day. Produced by averaging all temperature gradients from similar times of day over the 112 day deployment period.

290 degrees magnetic (approximately northwest), and a negative value indicates a current going towards 110 degrees magnetic (approximately southeast). A positive cross-shelf current is moving towards shore and a negative cross-shelf current value indicates offshore flow.

The 24 hour averaged cycles of alongshelf and cross-shelf currents at 12, 23, 34, and 45 m depth (figure 4.12) clearly contrast the two components. The alongshelf current at all depths shows a clear 24 hour period with an almost constant amplitude at the different depths of 2.0 ± 0.1 cm/s. The cross-shelf averaged temperature cycles all contain a component of semidiurnal period variability (probably caused by tidal internal waves), which increases with depth. At 45 m the cross-shelf current is almost perfectly fit by a 12 hour sine/cosine wave, while at 12 and 23 m there appears to be a combination of diurnal and semidiurnal period variability with better fits made with a 24 hour sine-cosine wave at both of these depths (table 4.4).

The phase of the 24 hour alongshelf current velocity averages remains almost constant with depth. In the demeaned averaged cycles, strongest currents down-coast are seen during the middle of the day and strongest upcoast currents are centered at midnight. The cross-shelf current velocities have considerably more variability with depth. The 12 and 23 m cycles are quite similar, but there appears to be a phase shift between these two positions and those calculated for the cross-shelf currents at 34 and 45 m. This apparent phase shift may in fact be a result of combined diurnal and semidiurnal variability in the near surface becoming more semidiurnal period

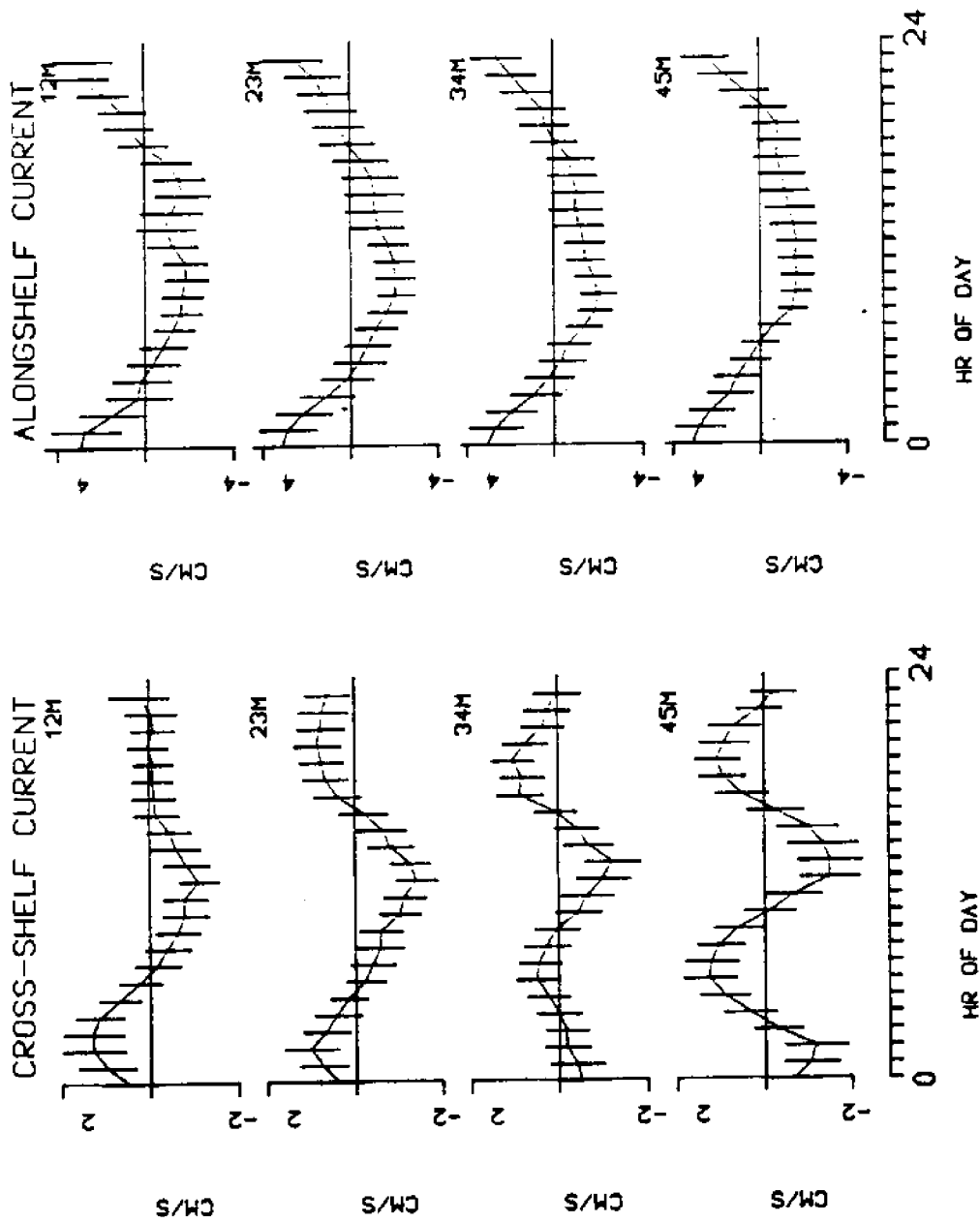


FIGURE 4.12 Averaged cycles of cross-shelf and along-shelf currents at 12, 23, 34, and 45 meters depth over a 24 hour day. All current data from the 113 day deployment period were used to develop these cycles. (Note: cross-shelf data are plotted with a velocity scale -2 to 2 cm/s, while along-shelf currents have a velocity scale -4 to 4 cm/s).

dominated at the deeper locations, and in fact maximum offshore currents at all four depths occur at the same time, centered on 12 noon. The 12 and 34 m averaged daily cycles of temperature also show a phase shift in the morning minimum and maximum temperatures which is almost the opposite of that seen in the currents. This is explained by comparing the averaged daily cycles of current and temperature directly. At 34 m the temperature cycle is 3 hours out of phase with the cross-shelf current cycle. As a result periods of maximum current velocity correspond to maximums in the derivative of the temperature cycle (i.e. periods of most rapid temperature change). Closer examination of these two cycles shows that temperature increases correspond to onshore current flow and temperature decreases correspond to offshore current flow. With maximum current values in the 34 m cross-shelf daily cycle of 1 cm/s (onshelf) and -1 cm/s (offshelf), and corresponding maximums in the derivative of the daily temperature cycle at 34 m of 0.05 °C/hr (1.4×10^{-5} °C/s), an estimate of cross-shelf horizontal temperature gradients at 34 m can be made. This value is 1.4 °C/km, (1.4×10^{-5} °C/cm), and is considerably higher than values calculated using the January hydrographic data (see above). The average magnitude of the tidal frequency variability in the currents and temperatures for the entire time series was significantly higher than the tidal frequency variability observed during the period in January when the hydrographic surveys were made. Thus it seems reasonable that the daily averaged cycles which used data from the full four month time series should indicate larger

horizontal gradients.

Figure 4.13 shows averaged current velocities and 95% confidence levels at 12, 23, 34 and 45 m for each month that the mooring was deployed. With the exception of May the cross-shelf current profiles are fairly consistent from month to month. The pattern seen is one of current velocities strongest onshore at 12 m and weakest at 45 m. Since for much of the spring, satellite images appear to indicate upwelling in the area it had seemed reasonable that, at least for some months the averaged currents would have been onshore at depth and offshore near the surface, in agreement with classical upwelling theory. However a small error in the rotation and separation of the current components would be enough to mask the features of upwelling which has a signal at least an order of magnitude less than tidal frequency current variability. The time scales of upwelling events (2-10 days) are such that monthly averages may average them out. From month to month, the alongshelf current profiles show much greater variability, although downcoast water movement is restricted to the upper layers. The overall average alongshelf current at 12 m is zero, but between 23, 34 and 45 m there is a trend of increasing net current velocity upcoast. A plot of the full four months of current data in the form of a progressive vector plot for each of the VMCM's shows close to 200 km of upcoast displacement of water at 45 m over the January to May period. Net cross-shelf displacement is about 100 km onshore at 12 m and decreases approximately linearly with depth with an almost zero onshore component at 45 m. These results do not support

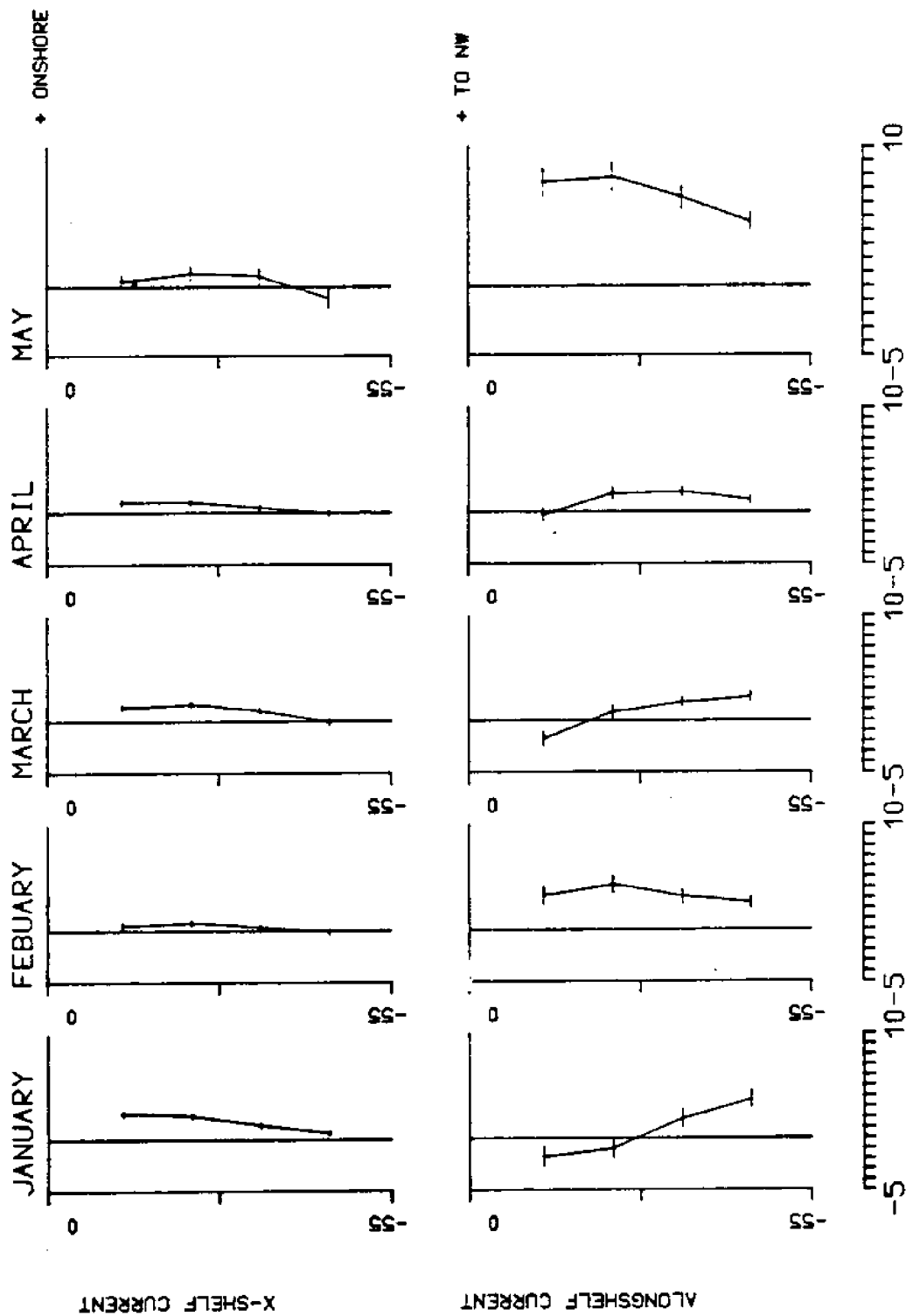


FIGURE 4.13 Monthly average velocity profiles through the water column for cross-shelf and along-shelf current components. Average current for each month of the deployment period is plotted for each sensor depth with 95% error ranges.

a two dimensional model of cross-shelf flow continuity, and raise the possibility of consistent, long term variation (in the alongshelf direction) of the cross-shelf flow regime. Perhaps some kind of small scale eddy formed by the unusual topography of the peninsula.

Comparison of the daily averaged cycles between the alongshelf and cross-shelf current components shows maximum alongshelf currents towards the northwest at all depths occur between 8 a.m. and 4 p.m., and correspond to maximum offshore currents in the cross-shelf component which are centered at midday. Maximum alongshelf currents to the southeast, centered for all depths at 12 p.m., correspond less closely to peak onshore currents which at 12 and 23 m are centered at 2 a.m. At 34 and 45 m, the cross-shelf current is in fact going offshore at 12 p.m.

Standard deviation estimates for the currents give values in the alongshelf component that are 2.5 times larger than for the cross-shelf component. This agrees with psuedo-drifter tracks used to prepare probability contours for water parcel trajectories near the mooring (figure 4.14). The contour lines in figure 4.14 are drawn to map out the 100 m by 100 m boxes into which a water parcel released at the mooring would end up some percent of the time after 3 or 6 hours, assuming horizontally constant currents. These contoured areas all show elongation in the alongshelf relative to the cross-shelf bathymetric axis. The occurrence of larger current magnitudes in the alongshelf relative to the cross-shelf co-ordinate is probably explained by flow continuity, (i.e. the steeply sloping shelf produces

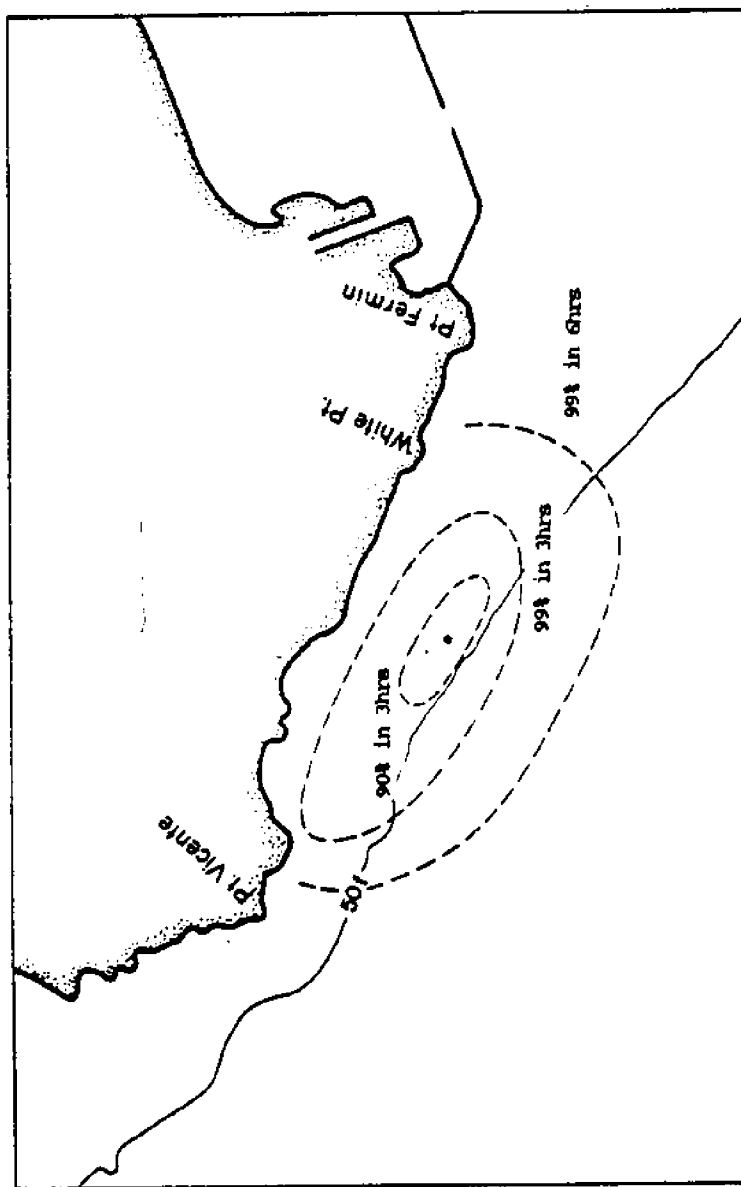


FIGURE 4.14 Histogram of the time integrated velocity histories derived from current velocities measured at the 12 meter sensor. The inner dashed line represents the boundary within which 90% of water parcels released at the mooring location would be contained after three hours. The middle dashed line is the boundary within which 99% of water would be contained after 3 hours, and the outer dashed line is the boundary within which 99% of water parcels would be contained after 6 hours. (A. Bratkovich, unpublished data).

an effective boundary to onshore moving water). Despite the larger magnitude of the alongshelf currents, at 12 m the mean value (based on a four month time average) is -0.11 cm/s. In contrast, the cross-shelf current at 12 meters has an overall mean value of 1.30 cm/s towards the coast. The ratio of the overall mean values of alongshelf to cross-shelf currents increases with depth.

PLATFORM BETA WIND DATA

Diurnal cycles in winds from the Platform Beta instrument (figures 4.15 and 4.16, see figure 1.2 for location of Platform Beta) interpolated from three hour instantaneous samples to hourly data using a linear interpolation, and rotated to the same alongshelf and cross-shelf angles used for the current data, are compared with the cycles seen in the temperature and current data. The demeaned alongshelf wind component has a maximum towards the northwest of 2.0 m/s at 7 a.m. and a maximum to the southeast of 1.3 m/s at 4 p.m. Thus alongshelf winds agree reasonably well with alongshelf currents at 12 m with an approximately 18 hour lagtime. The cross-shelf wind from Platform Beta has a maximum in the onshore direction of 0.6 m/s at 10 a.m. and a maximum in the offshore direction of 0.8 m/s at 7 p.m. The best fit of the cross-shelf wind with the daily cycle of the 12m current also falls at a lag time of 18 hours. In the northern hemisphere Ekman theory would predict near surface water to move in a direction about $45 - 90^\circ$ the right of the wind direction. With an 18 lag the daily cycles of current do seem to show water movement

AVG'D 24HR CYCLE OF AS WIND PLATFORM BETA

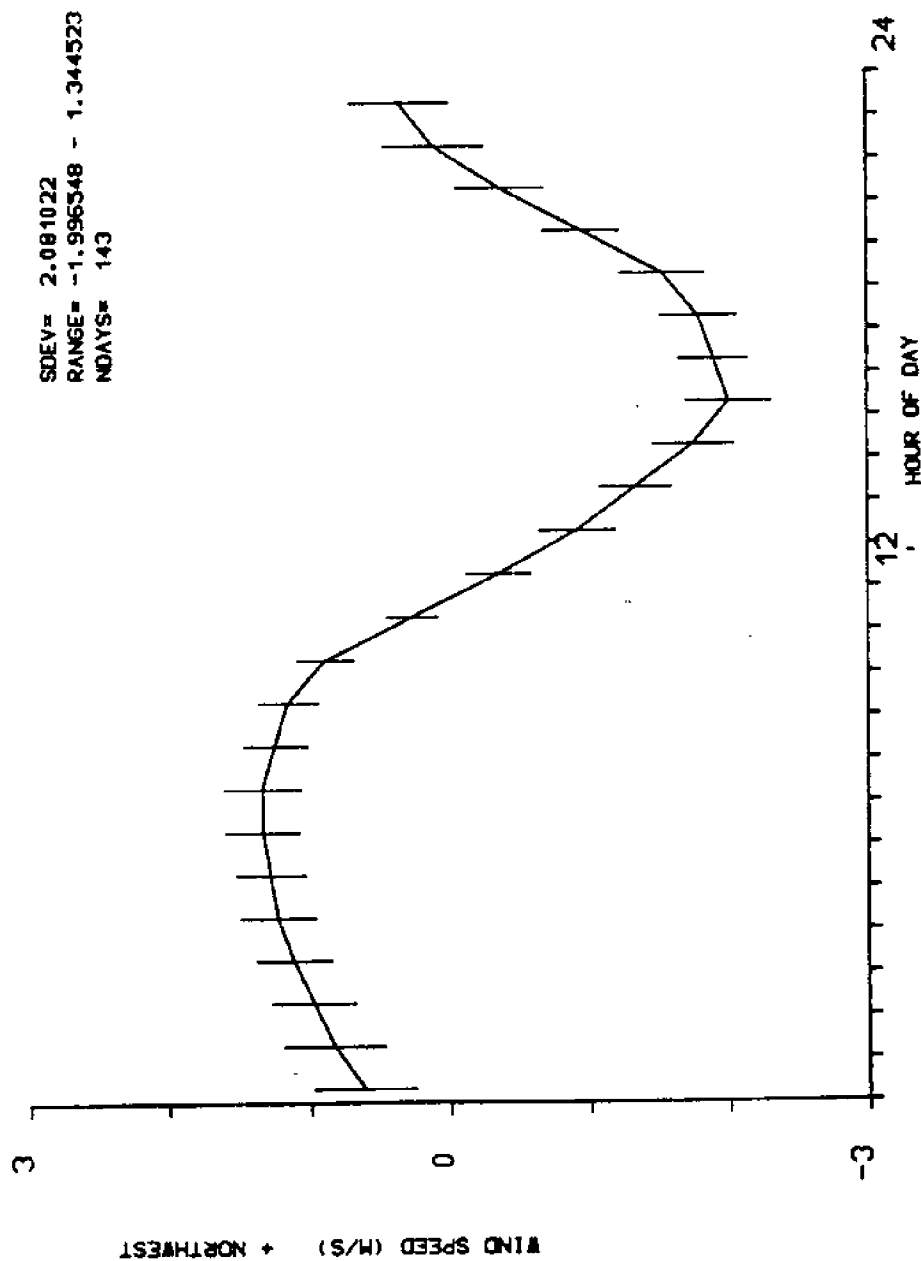


FIGURE 4.15 Averaged cycle of alongshelf wind measured at Platform Beta over a 24 hour day. Produced by interpolating original data from three hourly to one per hour values and then averaging all alongshelf wind speeds from similar times of day over the 143 day deployment period.

AVG'D 24HR CYCLE OF CS WIND PLATFORM BETA

SDEV= 1.4634
 RANGE= -.8010757 - .5868234
 NDAYS= 143

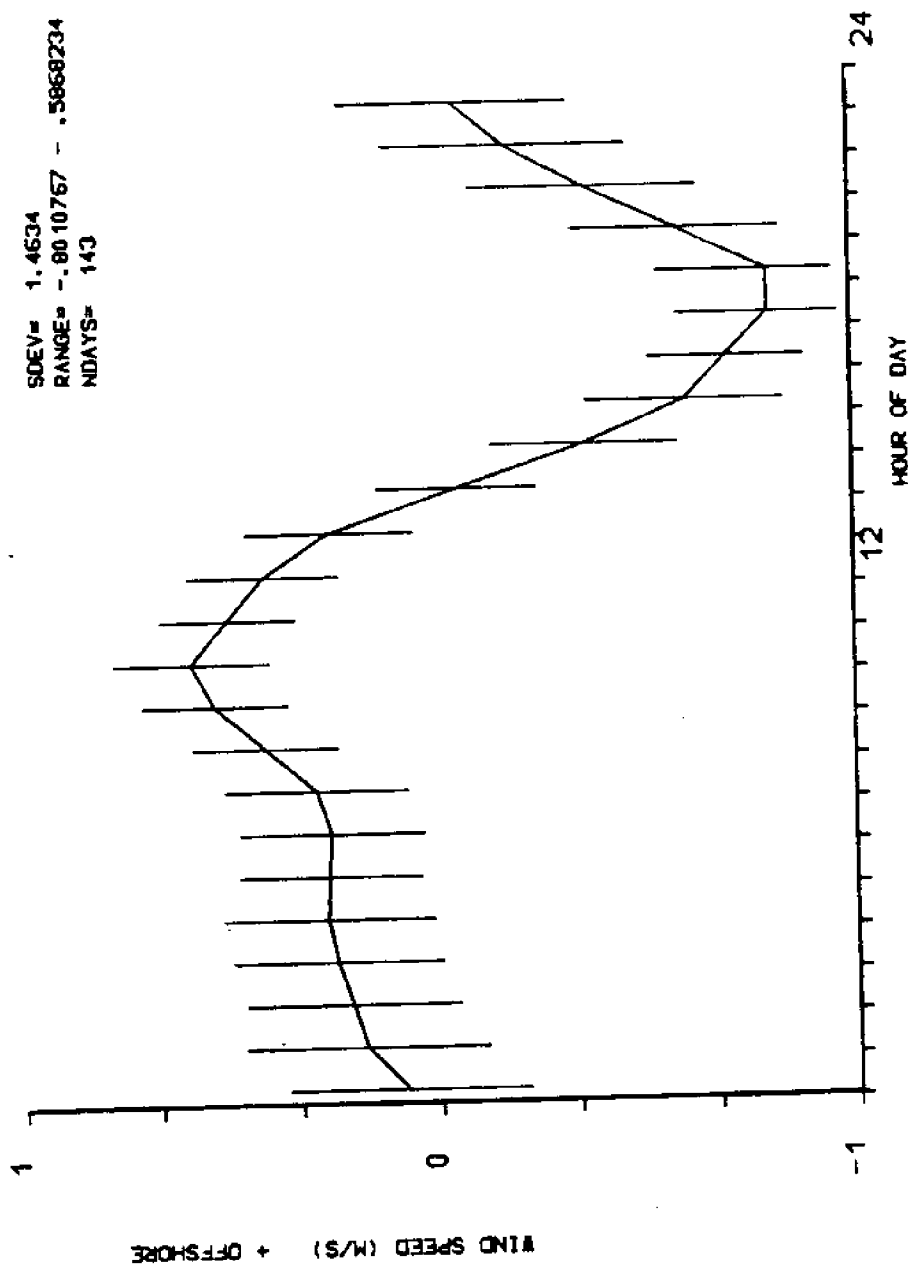


FIGURE 4.16 Averaged cycle of cross-shelf wind measured at Platform Beta over a 24 hour day. Produced by interpolating from three hourly to hourly values and then averaging all cross-shelf wind speeds from similar times of day over the 143 day deployment period.

downcoast and offshore, during the period of strongest wind towards the southeast in the daily cycle of alongshelf wind.

RELATIONSHIP OF TEMPERATURE TO THE EFFLUENT FIELD

The question of how the temperature field may modify the development of the effluent plume by determining the density stratification is complicated by the effect of the effluent upon the ambient temperature field. From the extensive hydrographic data set collected during the January cruises it was possible to construct a number of cross-shelf profiles. Figure 4.17 shows one of these cross-shelf sections repeated for temperature and for five other variables collected. In order to assess the relationships between the large number of hydrographic variables sampled a principal component analysis (see appendix for explanation of the principal component analysis) was used to identify linked groups of variables (Burton Jones et al., 1986 - in prep.).

Principal component analysis of the hydrographic data collected with the vertical pumping profiler on January 28 produced a first primary component with 46% of the variance which showed strong correlation of the temperature with chlorophyll, phaeopigment, nitrate, and silicate in a 'normal' oceanographic vertical structure where as temperature increases towards the surface the nutrient concentrations decrease and phytoplankton concentrations increase. The second component, with 24% of the variance, showed a strong correlation of salinity and sigma-t with phosphate, and ammonium. This

SG/LAC SECTION X=2 28-JAN-85

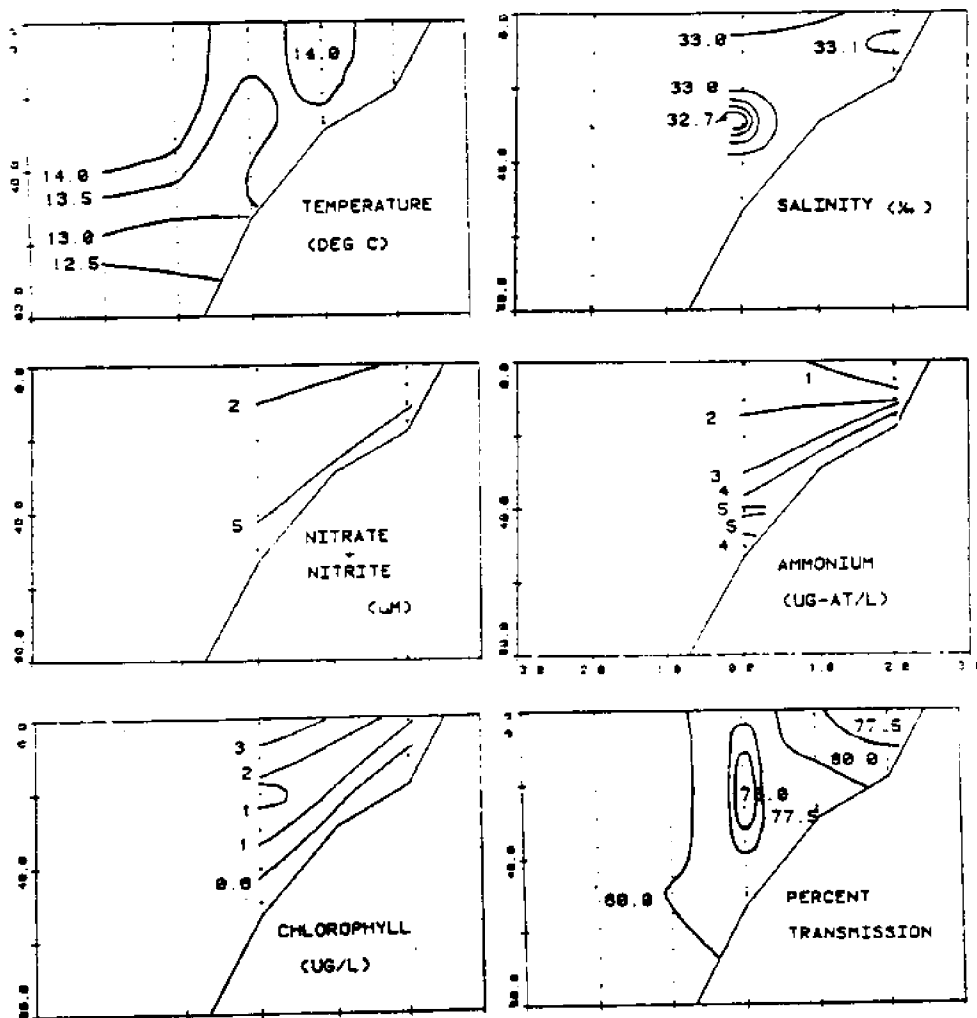


FIGURE 4.17 Typical cross-shelf hydrography section. Taken at grid location X=2 (see FIGURE 1), on the 28th of January 1985. (Burton Jones, unpublished data).

component which is identified by low salinity, low density water with high concentrations of phosphate and ammonium is believed to be indicative of the effluent field. When the scores for the two principal components are calculated and plotted on cross-shelf sections like those in figure 4.18 they clearly illustrate the different distributions.

Despite the apparent low correlation of temperature with the second, effluent driven component of variability, our cross-sections from some other days suggest that on occasion the temperature, and in particular, higher than ambient temperatures, may be effective indicators of the effluent field. A good example of this is seen in the cross-shelf section of temperature over the 3.04 m diffuser on January 23 (figure 4.19). LACSD hydrographic surveys have also found temperature to be an effective indicator of the effluent field in the winter when ambient temperatures are low and there is limited density stratification. The cross-section of temperature in figure 4.17 shows another pattern of temperature variation which seems to indicate an ambient temperature field/effluent field connection. In this particular cross-shelf contoured section of temperature the 13.5 °C isotherm is bent upward over the 60 m isobath. Although this cross-shelf line is displaced 1 km upshelf from the nearest outfall it seems probable that the rising effluent field is entraining cold water and carrying it towards the surface.

SG/LAC HYDRO LINE +2 1/28/85

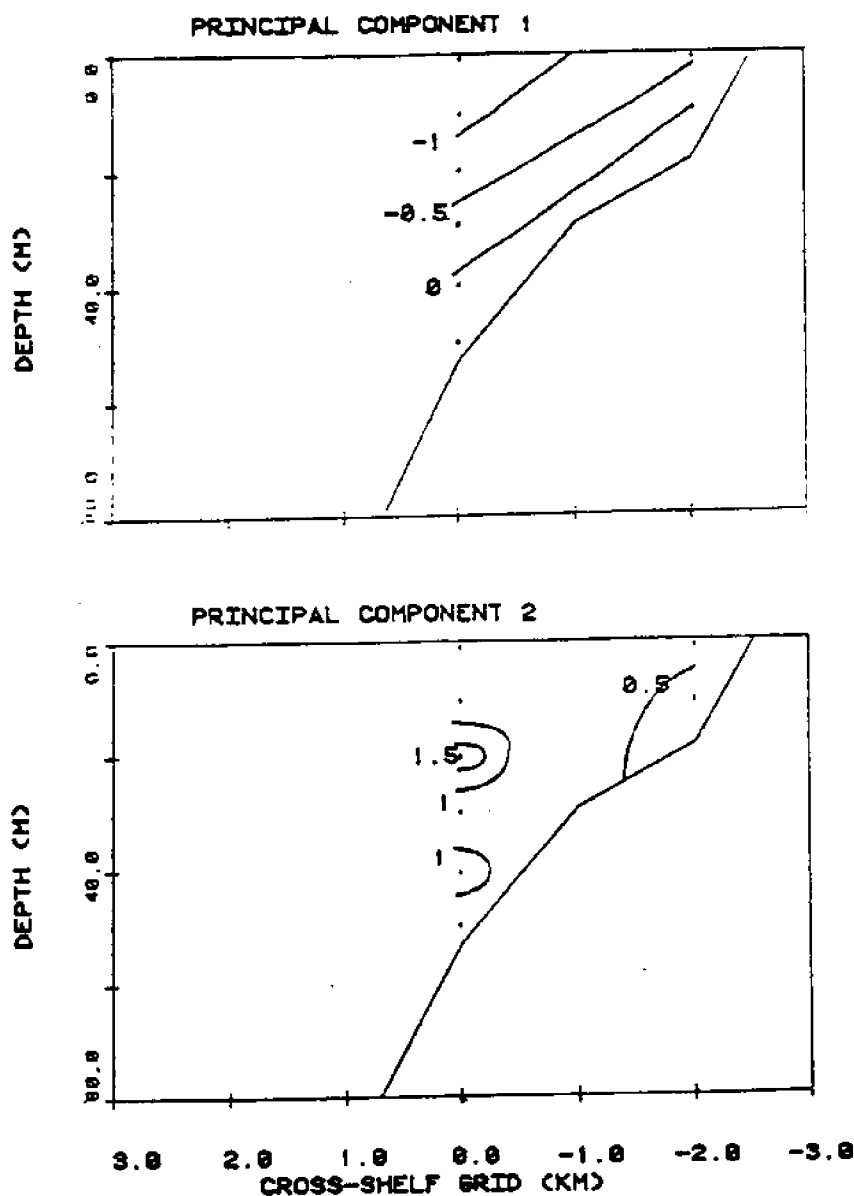


FIGURE 4.18 Distributions of the scores for the two principal components of variability identified in an analysis of the interrelationships between all the hydrographic variables sampled on the 28th of January. Principal component 1 apparently reflects the normal oceanographic stratification, with some sloping of the isopleths suggesting mild upwelling. Principal component 2 is characterized by high ammonia and low salinity and is believed to represent the effluent field. (see appendix for description of Principal Component analysis technique). (Burton Jones, unpublished data).

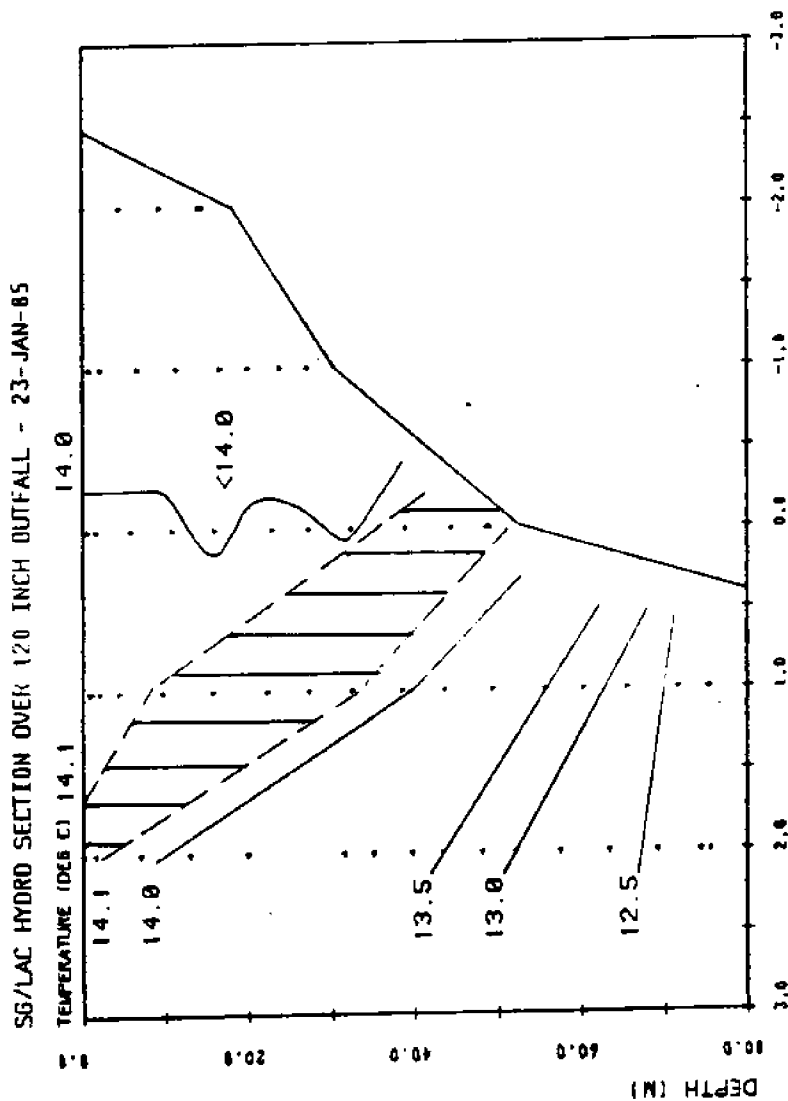


FIGURE 4.19 Cross-shelf section of temperature made over the 120 inch outfall diffuser on the 23rd of January 1985. Note the shaded area of temperatures > 14.1 degrees Centigrade. This probably indicates a rising effluent plume moving offshore and shows how on some occasions in the winter temperature can be a good indicator of the effluent plume. (Burton Jones, unpublished data).

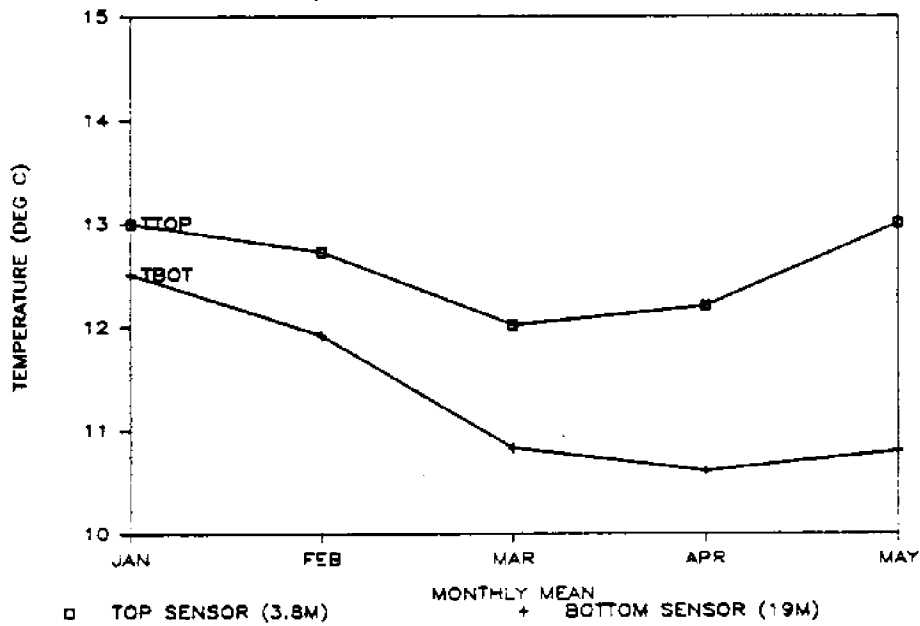
LACSD BUOY #1 DATA SET

Time series of temperature from the 4 and 19 m depth sensors on the LACSD buoy located in about 22 m of water seven kilometers southeast on the shelf from the USC mooring (see figure 1.1 for location) have been collected for the first five months of 1985. Time series and filtered time series were plotted for this period of the year, corresponding to the time when the USC mooring was deployed. Comparison of the temperature time series and the vertical temperature gradient, resultant signals show some similarities between the two moorings. Both have strong diurnal and semi-diurnal variability, and also show similar responses at event scales. Monthly statistics of the LACSD buoy data are plotted for the January to May 1985 period (figure 4.20).

SALINITY DATA

The salinity data collected during the January hydrographic cruises shows a very wide range in values, and it is likely that the area adjacent to the outfalls does indeed have a higher than normal variability in salinity (conductivity) due to the effluent input. Figure 4.21 is a temperature/salinity plot using all data from the January 28th hydrographic cruise. The absolute values of these salinity data are questionable, (it was necessary to add a constant of 2.0 to the original values in order to bring them into a realistic range based on historical environmental data) but the range of values is reasonable, judging from the behavior of the salinity data in the

MONTHLY AVG'D TEMPERATURES; LAC BUOY



MONTHLY ST. DEV. LAC BUOY #2

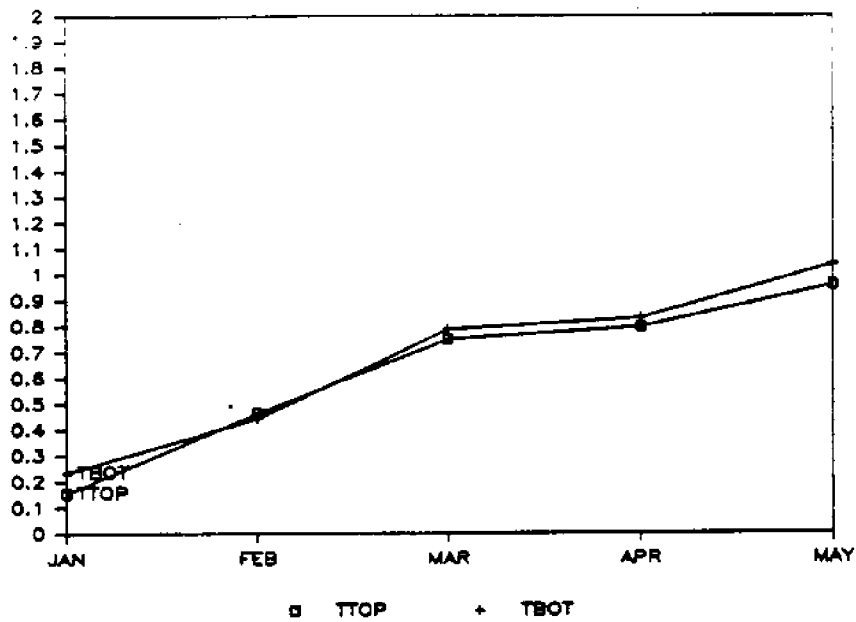


FIGURE 4.20 Monthly averaged temperatures (top), and standard deviations (bottom) for the 4 (TTOP), and 19 (TBOT) meter sensors on the LACSD mooring.

SG/LAC Hydrography

28 January 1985

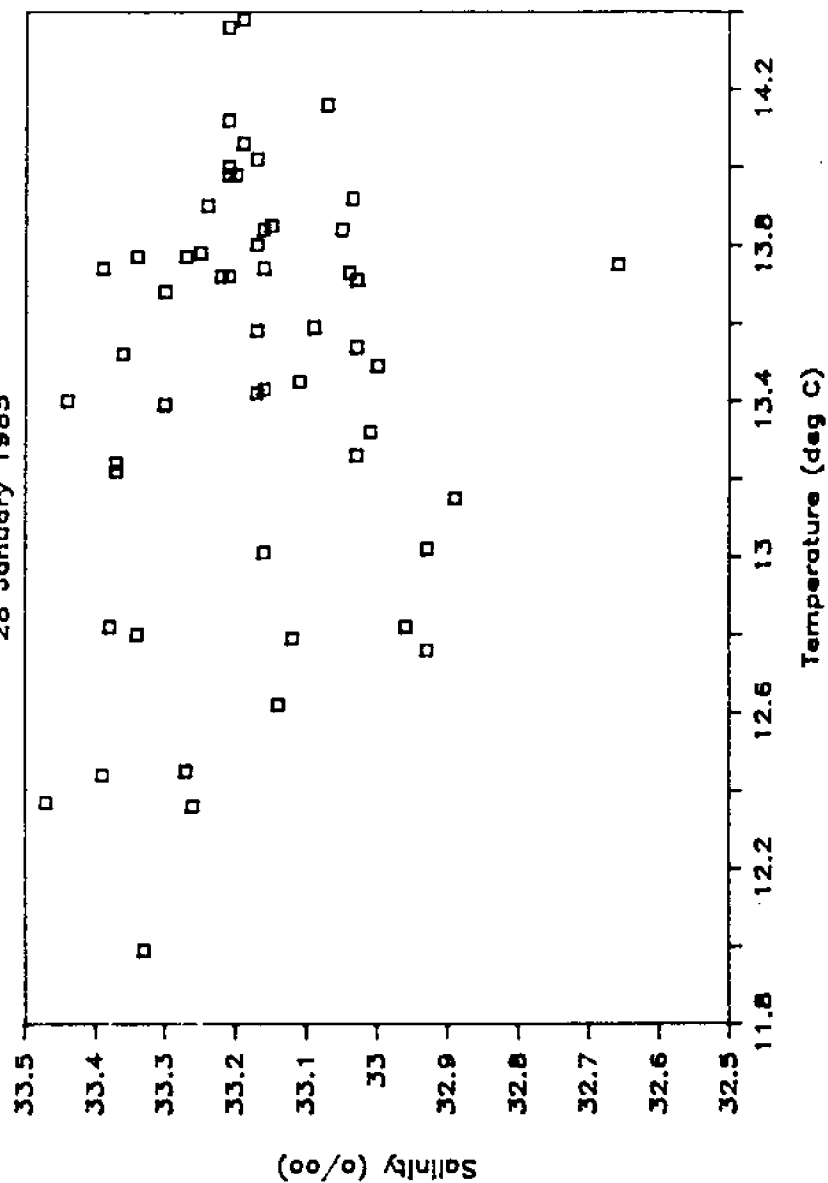


FIGURE 4.21 T/S plot of January 1985 data collected during hydrographic surveys on the Palos Verdes shelf. (Burton Jones, unpublished data).

principal component analysis. Calculation of the percent contribution to the density field variability by these temperature and salinity data was done using calculated standard deviations, and the same formula used for the historical data sets. Results show that on January 28 about 55% of density field variability was due to temperature variability and 45% was due to salinity variability. Salinity data available from the LACSD also show a range of values significantly greater than would be anticipated by CalCOFI data (see below). Without a time series of salinity data, the calculations of sigma-t must use these temporally intermittent hydrographic observations.

CALCOFI AND PIER-END HISTORICAL RESULTS

California Cooperative Fisheries Investigation surveys of the Pacific coast which have been in progress since 1950. They provide a set of valuable statistics for the temperature, salinity and sigma-t fields for our general study area. Data from the CalCOFI records have been collected from the two nearest inshore stations in the CalCOFI station plan. The first is station 35 on line 87 which is located offshore of Santa Monica Bay, and the second is station 28 of line 90 which is located offshore of Huntington beach (see figure 1.2 for locations). Figure 4.22 shows plots of the monthly averaged temperature and salinity data for 20 years worth of CalCOFI hydrographic profiles at line 90, station 28 at a depth of 10 meters, and the monthly averaged temperature and salinity for a continuous 10

CALCOFI 90028

SAN CLEMENTE

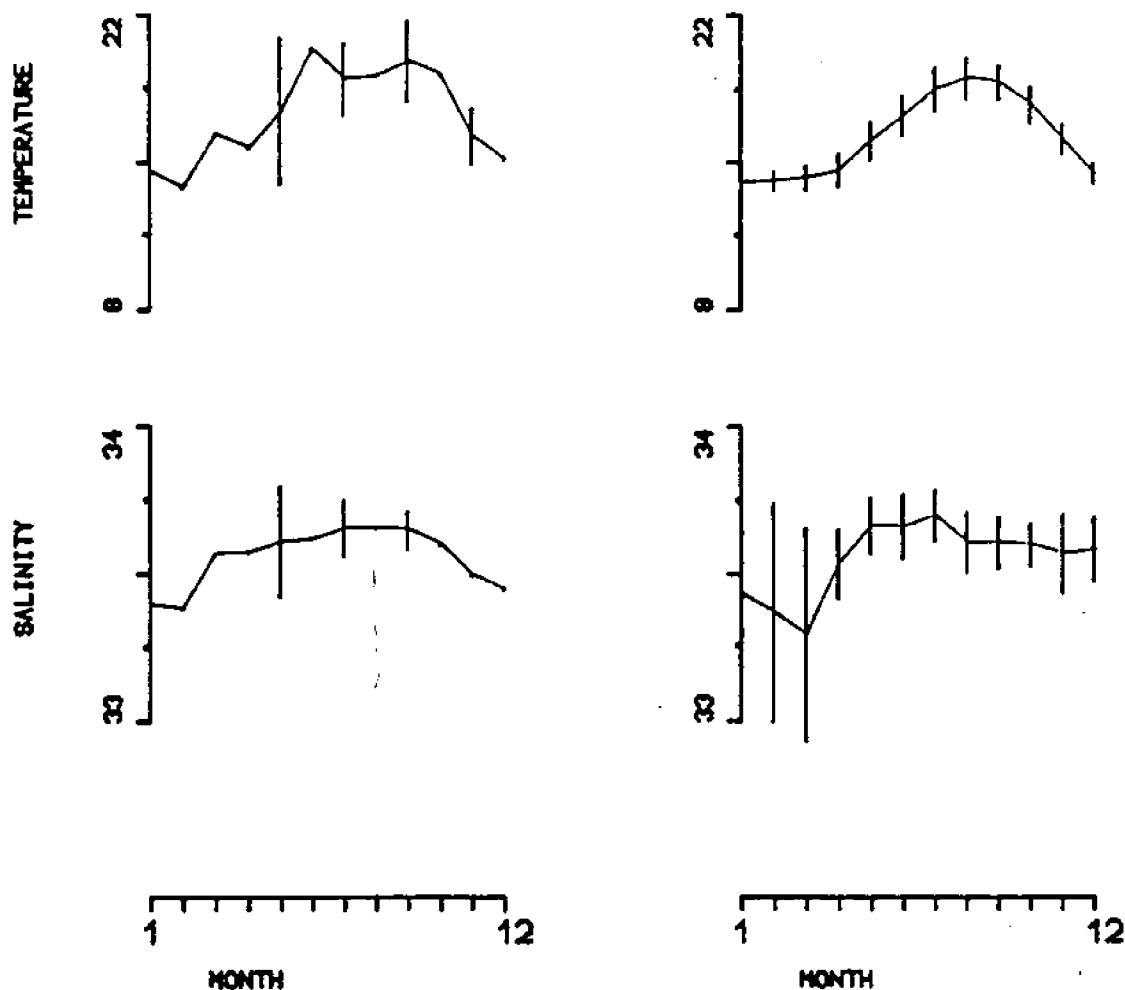
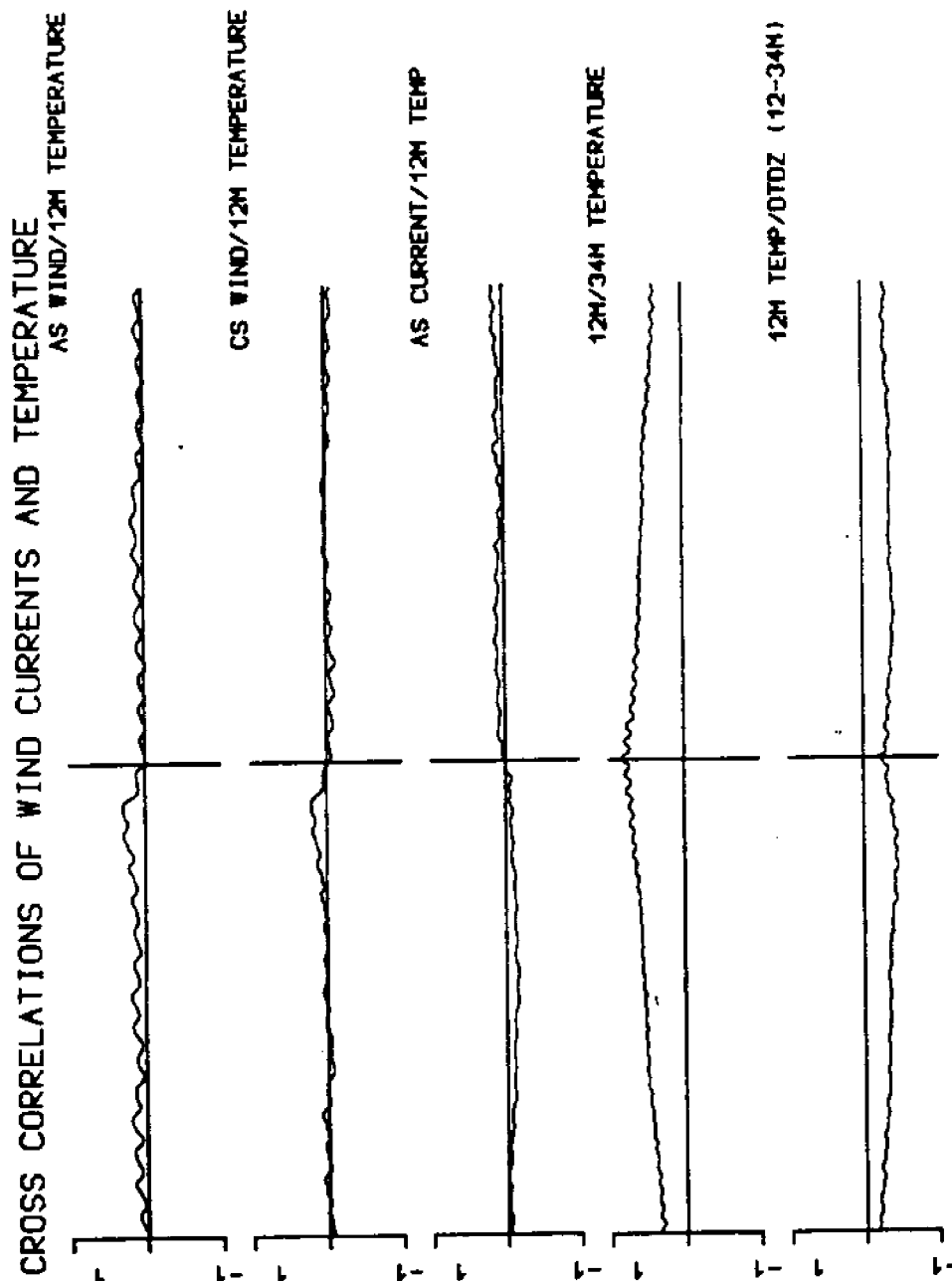


FIGURE 4.22 Monthly averaged temperatures and salinities for 20 years of CalCOFI data at line 90 station 28. 95% confidence intervals are shown only for the months which were sampled on at least four separate occasions. Also ten year average of San Clemente monthly average pier-end temperatures and salinities. Low salinities and large 95% confidence intervals for January, February and March reflect the effects of wintertime storms and freshwater run-off on the nearshore pier-end data.

year set of pier-end data from San Clemente. 95 percent confidence level bars for the CalCOFI data from line 90 station 28 are shown only for those months where more than three separate data points exist. Both the CalCOFI and the San Clemente pier-end annual cycles of temperature show net increases in temperature between January and early May (+1.2 °C at CalCOFI station 90028 and +0.5 °C at San Clemente pier). A midwinter warming feature, such as is identified by List and Koh (1972) in studies of long term data sets in the southern California bight, can not be seen in the 10 year average of San Clemente pier end data in figure 4.22. However this midwinter peak is only a small fraction of the annual signal and the position of the peak varies from year to year. A ten year data set such as that from San Clemente may have averaged this feature out. The CalCOFI data for station 90028 seem to show a warm peak during March, but this month was sampled only once in the 20 year record, and could reflect an unusual year.

CROSSCORRELATION ANALYSIS

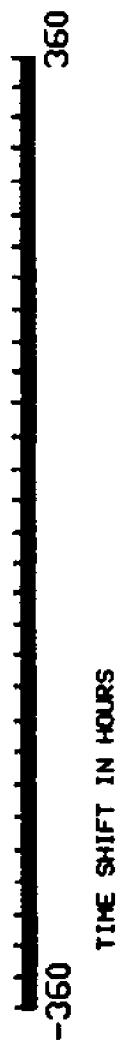
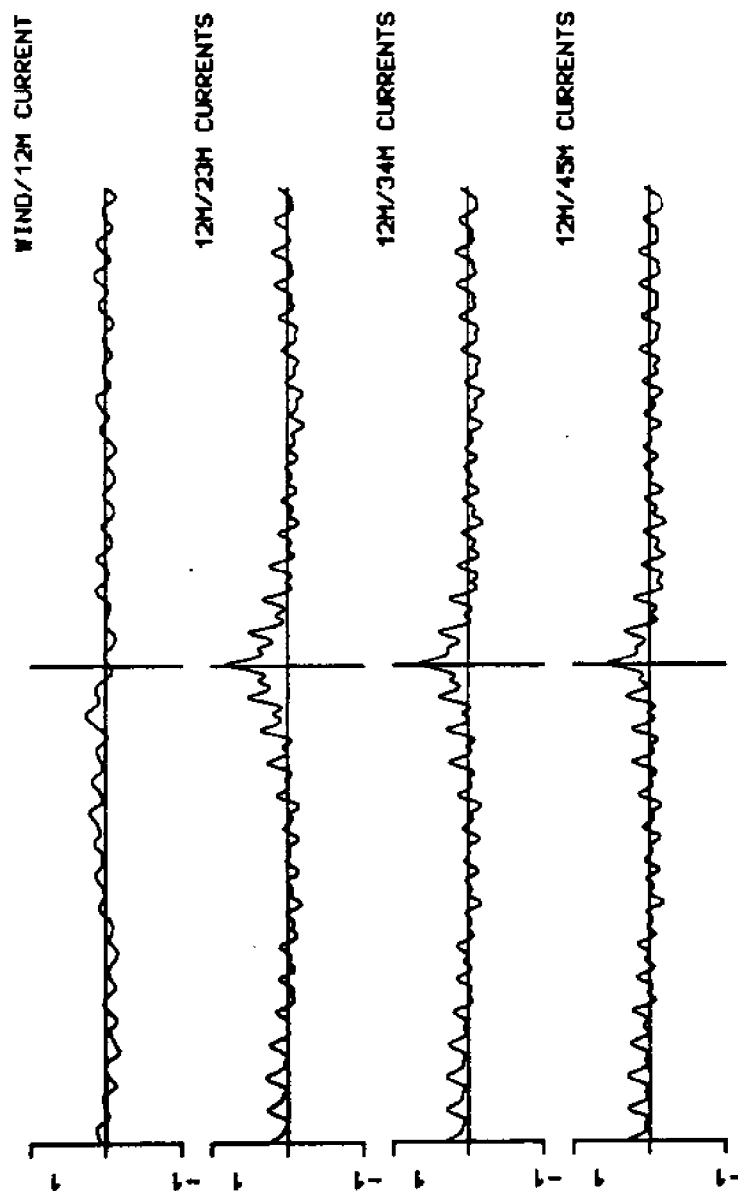
Figure 4.23 shows the results of a number of crosscorrelations made between the the different variables which were collected during this study. Time lags range from -360 hours (15 days) to +360 hours. Correlations between wind components and currents, between wind and temperature, and between current and temperature are all low, even at zero time lags. The six hour lag between wind and current seen in the daily cycles does not appear in the crosscorrelation. Currents at different depths have reasonably high (greater than 0.5)



-360 TIME SHIFT IN HOURS 360

FIGURE 4.23 Cross-correlations between winds, currents, and temperatures. Cross-correlations were carried out for a range of time lags from -360 hours (15 days) to +360 hours. (Continued on next page).

CROSS CORRELATIONS OF ALONGSHELF WIND AND CURRENTS



crosscorrelation values at time lags from -3 to 3 hours. Crosscorrelation of temperature at 12 m with temperature at 34 m produces values greater than 0.5 for time lags of up to a week, however temperature data were not detrended and crosscorrelation results may be larger as a result.

SATELLITE SEA SURFACE TEMPERATURE IMAGERY

Figure 4.24 is an infra-red satellite image of the southern California bight centered on the Palos Verdes peninsula. This image was taken by the NOAA-9 satellite and the color enhanced sea surface temperature picture was prepared by Dr. Gary Kleppel at the Scripps Institution of Oceanography Satellite Facility. This picture is representative of the sea surface temperature conditions which existed during the spring of 1985 (G. Kleppel, personal communication). Notable features in figure 4.24 are the cold water immediately adjacent to the coastline off Palos Verdes Peninsula (relatively cold water is shown in blue) and also to the north in Santa Monica Bay and south of Point Dume. This cold water is believed to be the result of localized upwelling bringing cold subsurface waters shoreward and to the surface. Just south of the peninsula is a shallow area of shelf which extends up to 10 km offshore. The large harbor complex of Long Beach is located at this point on the coast, and the nearshore area, enclosed by a breakwater, which shows up as a "pool" of warm water is a regular feature.



FIGURE 4.24 Infra-red satellite image showing typical sea surface temperature field for Spring season off Palos Verdes peninsula. Bluest water is coldest. Apparent upwelling is indicated by nearshore cold water just off southern coast of the peninsula. Pixels in this image are approximately 1.1 km on a side. This image was taken on April 26, 1985. (G. Kleppel, unpublished data).

5.0 DISCUSSION

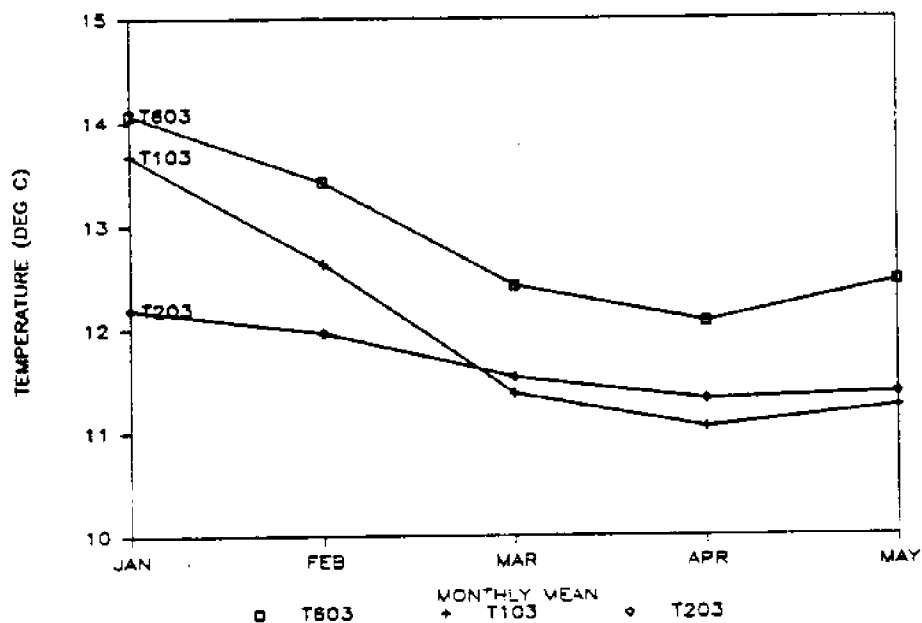
COMPARISON WITH HISTORICAL RECORDS

The temperature data obtained between January and May of 1985 at the 12 and 34 meter sensors on the USC mooring have been compared with the long term data sets of the CalCOFI program, and the pier-end data collected at numerous points along the coast since the early part of the century.

CalCOFI data from line 90 station 28 and line 87 station 35 collected between 1952 and 1972 were used to produce monthly averages of temperature and salinity. Pier-end data for a continuous ten year period from San Clemente were also gathered and averages were made for each month over the ten years. Plots of the monthly averages of temperature from CalCOFI line 90 station 28 and from San Clemente (figure 4.22) can be compared with the monthly averaged temperatures from the moorings (figure 5.1). The results indicate either that this was an anomalous year or that this is a special location. During the first four months of the year temperature dropped by over 2 °C, while both the CalCOFI and San Clemente temperature averages show a net increase in temperatures over the months January to April.

List and Koh (1976) identify a consistent mid-winter temperature peak in their study of southern California pier-end data, but this is missing both from our mooring temperatures and from the ten year average of San Clemente temperatures. This mid-winter peak in temperature is only a small fraction of the amplitude of the annual signal and shifts its position by up to two months from year to year,

MONTHLY AVG'D TEMPERATURES; SG/LAC



MONTHLY ST. DEV. SG/LAC BUOY

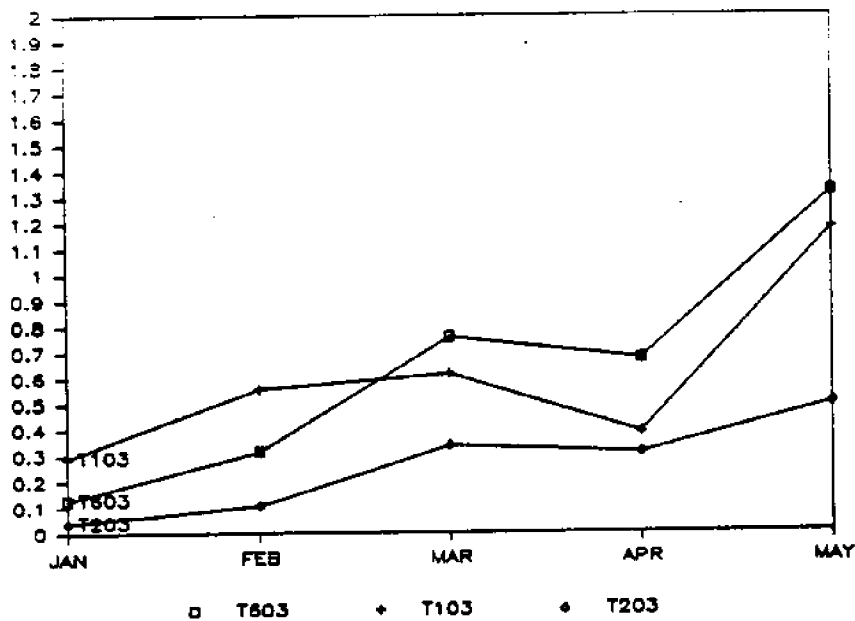


FIGURE 5.1 Monthly averaged temperatures (top), and standard deviations (bottom) for the 12 (T603), 23 (T203), and 34 (T103) meter sensors on the USC mooring. Note that the 23 meter data (T203) are not in agreement with the 12 and 34 meter means and standard deviations.

for this reason it is probably averaged out of the ten year average from the San Clemente pier. An apparent peak in the winter temperature in the CalCOFI averaged data from station 28 on line 90 in March is most likely explained as being due to the fact that this month was sampled only once in the twenty year period over which data were averaged and may represent an unusual year. These CalCOFI temperatures use only the surface measurements. Additionally the CalCOFI monthly averages are influenced by the fact that each month was sampled only on a few of the possible 20 years, and so year to year variability such as that occurring during El Nino events may produce large anomalies in adjacent months of averaged temperatures. An examination of the monthly averaged, contoured sea surface temperature maps prepared by the Naval Oceanography Command Detachment (1983), suggests that in January, February and March monthly averaged surface temperatures off Palos Verdes were nearly constant at 14.4°C , and that in April they rise to 15°C and in May to 16.1°C . These temperature values were interpolated by eye from large scale contoured sea surface temperature maps which may not have been contoured at a high enough resolution to show localized upwelling regions.

The drop in water temperature observed in the first four months of 1985 on the shelf off Palos Verdes does not seem to be explainable as a phase shift in the mid-winter warm peak described by List and Koh (1976). Although this peak does move by up to two months between annual cycles (the mid-winter temperature peak can occur anywhere between February and April), it has a magnitude of less than 1°C , and

times from the peak of the mid-winter warming to the onset of spring warming are less than two months. Further the mid-winter peak is superimposed on the the larger scale annual cycle which usually shows a net warming over the first four months of the year.

Perhaps the most likely explanation for the decrease in temperature on the Palos Verdes shelf during the first four months of the year is provided by IR satellite images of the Southern California Bight which show, particularly in March and April, frequent occurrences of cold nearshore water off the southern portion of the peninsula (see figure 4.24). It is believed that these images indicate enhanced upwelling in this area, such as is also observed off other promontories farther north. Huyer (1977) identifies a summer minimum in the temperature on the shelf off Oregon which she believes is a result of enhanced wind driven upwelling during the summer season bringing colder water to the surface. It is quite possible that a similar process produces a spring temperature minimum in waters off the Palos Verdes Peninsula. With only one year of temperature data the possibility that winter and spring of 1985 were anomalous can not be ruled out, and January of 1985 was an unusually warm month. Even if the spring temperature minimum we observed is a consistent feature it is still very localized, since multiyear records from nearby areas show rising temperatures in the period January to April. Satellite images for the spring of 1985 show that relatively strong localized apparent upwelling around Palos Verdes was limited to the southern edge of the peninsula and that the nearshore cold water plume extended

only for a few kilometers offshore.

TEMPERATURE/SALINITY CONTRIBUTIONS TO DENSITY

From analysis of the levels of variability in the temperature and salinity data in the averages for each month from both the CalCOFI and the pier-end data sets an estimate was made of the average percent contribution to the density variation, by temperature and salinity (in any given month). These percentages were calculated using the standard deviations of the temperature and salinity produced from each monthly average put into a linear equation of state which assigned a linear factor to each in terms of its influence on the density. Results from the CalCOFI data suggest that, in winter, temperature contributes about 60-70% of the density variation, with the remaining 30-40% due to salinity changes. In summer months, and in early fall, the salinity contribution drops to ~10%. The pier end data results show temperature contributions of 50-60% in winter and about 80% in summer. Some of the differences between these results can be explained by the fact that the pier end salinity data have higher standard deviations due to storm events producing relatively large influxes of freshwater into nearshore regions, particularly in the winter months. The salinity can be seen to drop in the first 3 months of the year at San Clemente (figure 4.22). These months also have the largest 95% confidence levels. The CalCOFI stations are further offshore and are not influenced by these fresh water influxes during storm events. However since the CalCOFI data are intermittent and spread over 20 years the

standard deviations produced for each averaged month may reflect interannual differences such as those related to El Nino events where the year to year differences in temperature may be much larger than in salinity.

These percentages seem to agree with the observed temperature driven highly stratified summer environment, but suggest that in winter months when density stratification is much weaker the role of salinity in defining the stratification may become much more significant. Huyer (1977) examined a large amount of hydrographic data collected on the Oregon shelf, and concludes that both temperature and salinity are significant in determining sigma-t values. Winant and Bratkovich (1981) state that typical density changes due to temperature fluctuations are 2-3 times larger than those associated with salinity fluctuations (i.e. temperature accounts for 66-75 % of density variation) observed in a set of mooring data from the shelf off of southern California. Their results used data for all seasons of the year.

The temperature/salinity results in figure 4.21 suggest that the effluent field contribution to salinity variability in the vicinity of the Whites Point outfalls is significant and probably plays a considerable role in defining the local density stratification. With the same linear equation of state used above salinity was calculated to be responsible for 45% of the density variability in this data.

TRENDS IN TEMPERATURE DATA

During the 113 days of the current meter deployment, beginning on January 14th and ending on May 9th, there was, for at least the first 100 days a fairly steady decrease in the temperatures at both the 12 and 34 meter sensors. This can be seen in both the 15 day filtered time series and in the plots of monthly averaged temperatures. List and Koh in their analysis of pier end data identified a mid-winter rise in the temperature which seems very persistent from year to year. This is not apparent in our temperature record, and in fact even without the mid-winter rise in temperature that they observed, the pier-end records examined by List and Koh seem to show increasing temperatures over the same period where our temperatures drop by 2 °C. The ten year averaged cycle of pier-end temperatures from San Clemente (figure 4.22) shows no mid-winter rise, but does in fact increase steadily between January and May.

During the first four months of 1985, even though the temperature on the shelf off Palos Verdes was decreasing, there was a moderate increase in the monthly average vertical temperature stratification. This can be explained by examining the monthly probability density plots of the temperature at 12 and 34 m and the temperature gradient (Figure 4.7). The April and May probability density distributions for the 12 m temperature and the temperature gradient are broader and more flattened than the distributions for the 34 m temperature, indicating the intermittent development of higher near surface temperatures in a mixed layer shallower than 34 m. The slightly skewed distribution of

the 34 m temperature probability density for May towards higher temperatures probably reflects occasions when the mixed layer reached below 34 m.

Increases in the levels of variability observed in the temperature, temperature stratification and currents between January and May can be seen both in the increasing amplitude of the high frequency signal isolated from the temperature signal (table 4.1), and in the plot of monthly standard deviations of the temperature (figure 5.1). This seems to indicate that the environment was gradually becoming more energetic throughout this period. Although it is not clear whether this is the result of increased solar radiation, seasonal changes in large scale current systems, or increased wind and tidal forcing. It is also possible that as the seasons change there is a reorganization of the most energetic frequency bands. Bratkovich (1985) has compared energy spectra plots for the different seasons and has also noted the increased variance levels at diurnal and semidiurnal frequencies in summer relative to winter (variance levels increased by up to two orders of magnitude in summer).

Of significance to the fate of the effluent plume is the seasonal change in the vertical density gradient. The 15 day filtered time series of the temperature gradient, (calculated using a finite difference estimate between 12 and 34 meters) shows a gradual increase between January and May. Without salinity data it is difficult to be certain of the degree to which the density gradient evolution agrees with the temperature gradient signal, however if estimates of the

percent of density variability due to temperature (made using CalCOFI and pier-end records from nearby locations) are considered, then for winter months somewhere between 60 and 70% of the density gradient is derived from temperature stratification.

CROSS CORRELATIONS OF WINDS, CURRENTS AND TEMPERATURES

Figure 4.23 shows crosscorrelation results for a number of comparisons between different variables. Alongshelf wind from Platform Beta has a very low correlation with the 12 m depth, alongshelf current, even at zero time lag (less than 0.1). Correlations between the alongshelf component of the currents at different depths on the mooring show reasonably high values for only the first 2 to 4 hours (at zero time lag, values range from 0.5 - 0.8). Correlations between winds and temperatures at 12 m and between the current and temperature at 12 m are all low even at zero time lag (all values are less than 0.1). The correlation of the 12 and 34 m temperature records is quite high, with values greater than 0.5 at time lags of up to a week, however the temperature data were not detrended and this may have influenced the results for this crosscorrelation.

DIURNAL AND HIGHER FREQUENCY VARIABILITY IN CURRENTS AND TEMPERATURES

Power spectra of the current and temperature time series from our mooring (figure 4.5) agree with similar analyses made by several earlier researchers (List and Koh, 1976, Winant and Bratkovich, 1981,

Bratkovich, 1985). The local maxima in energy density levels are observed at tidal frequencies of 1 and 2 cycles per day. This result has unfortunate implications for any attempts to design a predictor model of the currents or temperature, since, in addition to this high frequency variability crosscorrelations between winds, currents, temperatures and the temperature gradient all fall to low levels within only a few hours (figure 4.23). A qualitative comparison of the four month time series of temperature from the mooring with wind records from nearby stations indicates that certain wind events (e.g. strong winds blowing towards the southeast for longer than 24 hours) may have more predictable effects on the temperature field.

Hydrographic surveys which take up to 12 hours to complete are subject to aliasing effects by high levels of variability at tidal time scales. When the plot of standard deviations of the monthly averaged temperatures from the sensors at the mooring is examined and compared with the average temperature gradient values, it is apparent that vertical displacements of the temperature isopleths of several meters are occurring at diurnal and semidiurnal frequencies. The magnitude of the high frequency temperature variability, seen in figures 4.3 and 4.4, was very low during the last two weeks of January, as was the high frequency variability in the current components. For this reason it can be assumed that January 1985 hydrographic data is relatively free from tidal frequency distortions.

An extensive set of cross-shelf contoured cross-sections was prepared from the data sampled during the 7 hydrographic cruises made

in January 1985. The temperature cross-sections indicated that there is considerable day to day variation in the stratification, both in the vertical movement of isopycnal surfaces at a set location, and in the slope of isopycnal surfaces across the shelf. As expected some disruption of isopycnal surfaces was seen over the diffusers (due to entrainment of water by the rising effluent), but additionally there were consistent alongshelf and depth related patterns in the slopes of isopycnal surfaces, on some days these were observed to slope upward toward the coast and on others to slope down towards shore.

TRENDS IN CURRENT DATA

The monthly averages of the alongshelf current velocities from the mooring show relatively small magnitudes, and except at the 12 m VMCM these small net currents are all towards the northwest. These average currents agree with geostrophic currents given in the Climatic Study of the Southern California Operating Area which range from 0.5-2.0 cm/s towards the north for the months January to May. Both Hickey (1979) and Tsuchiya (1980) report results of earlier current and drifter studies in the northern half of the Southern California Bight which show southerly currents in April. Our results show the only southerly currents between January and May 1985 occurred in January and March, and then only at the 12 m VMCM. Flow at the deeper instruments was always to the northwest. The standard deviations calculated for the alongshelf and cross-shelf components of the current do seem to indicate that the alongshelf component is

considerably more energetic. Comparison of the spectra for these components, as well as the high and low frequency variability signals shows that despite the difference in magnitude the distribution of variability with frequency remains similar between the alongshelf and the cross-shelf components.

Cross-shelf average profiles of current velocities at 12, 23, 34 and 45 m are considered with respect to satellite SST imagery which shows the frequent occurrence, particularly in March and April, of cold surface water immediately adjacent to the peninsula. This is assumed to represent upwelling and it seemed possible that the VMCM current measurements would have reflected the upwelling process by producing average currents in the offshelf direction near the surface and onshelf at the deeper instrument locations. One explanation may be that the offshore moving water was confined to the very near surface layers, above the shallowest VMCM at 12 m depth. It is also possible that the topography of the peninsula produces a pattern of cross-shelf flow such that water moves onshore at one point and moves offshore at another point up or downcoast. Upwelling and downwelling related currents are part of a secondary circulation pattern with average magnitudes that are typically 1 to 2 orders less than tidal frequency variations and other subinertial contributions. Winant and Bratkovich (1981) were unable to isolate any mean cross-shelf circulation patterns on the shelf off Del Mar California using a similar set of cross-shelf and alongshelf current data.

DISCUSSION OF SIGNIFICANCE OF DAILY AVERAGED CYCLES

Because of the difficulty in relating the different variables measured during this project directly, averaged daily cycles were used as one method of isolating and identifying relationships between variables. Daily averaged cycles are of particular applicability to this study because of systematic daily variability in the flow rates of effluent from the JWPCP treatment plant to the diffusers on the shelf, and because of the coliform monitoring procedure which occurs at a fixed time each day. Also, two important variables which drive the temperature field on the shelf, solar insolation and wind stress have strong daily cycles.

In the case of the Platform Beta winds the averaged cycles of cross-shelf and alongshelf winds tend to filter out event scale variability of 2-10 day duration. For the current and temperature cycles, not only has event scale variability been averaged out, but also several tidal constituents that are not phase locked with the 24 hour day. The range of the resulting cycles thus is a fraction of the typical range of the signal seen in any randomly selected 24 hr period. Nonetheless, the 95% confidence levels calculated using the standard deviations of the average values for each hour from the 113 day records, plotted on these averaged 24 hour cycles seem to support their validity (on average the range of the 95% confidence levels is only one fourth or less of the range in the corresponding averaged cycle) and some reasonable correlations of minima and maxima in these cycles between different variables can be seen.

Figure 5.2 is the averaged 24 hour cycle produced from the sea surface elevation signal interpolated to hourly values for the first 5 months of 1985. It shows good agreement with the averaged cycles of temperature from the 12 and 34 m sensors. Using an overall average temperature gradient value of $0.04^{\circ}\text{C}/\text{meter}$ and considering the total range in the averaged cycle of sea surface elevation is roughly 0.6 m and that the range of the temperature cycles at both 12 and 34 m depth is $0.3 - 0.35^{\circ}$ it can be seen that the passive shift of isotherms past the sensors as the sea level changes should on average only be responsible for about 10% of the observed average daily temperature variability. This suggests that internal tidal waves such as were observed by Liepper (1955) are present on the Palos Verdes shelf. One component of these internal tidal waves seems to drive the movement of temperature isopleths so as to keep them in phase with surface tides, since maxima and minima occur at the same points in the daily averaged cycles for the 12 and 34 m temperature and the surface tides. The 34 m daily cycle of temperature is observed to be about 3 hours out of phase with the daily cycle of the 34 m cross-shelf current. This results in maximum rates of temperature increase at 34 m of $1.4 \times 10^{-5}^{\circ}\text{C}/\text{sec}$ occurring during periods of maximum onshore current velocities (about 1 cm/sec). Rates of temperature decrease are similar to those for temperature increase and correlate with peak offshore current velocities which are also about 1 cm/sec.

AVG'D 24 HR CYCLE OF PREDICTED TIDES

MEAN= -3.670559E-08
 SDEV= 1.622636
 RANGE= -1.311072 ~ 1.060214
 NDAYS= 148

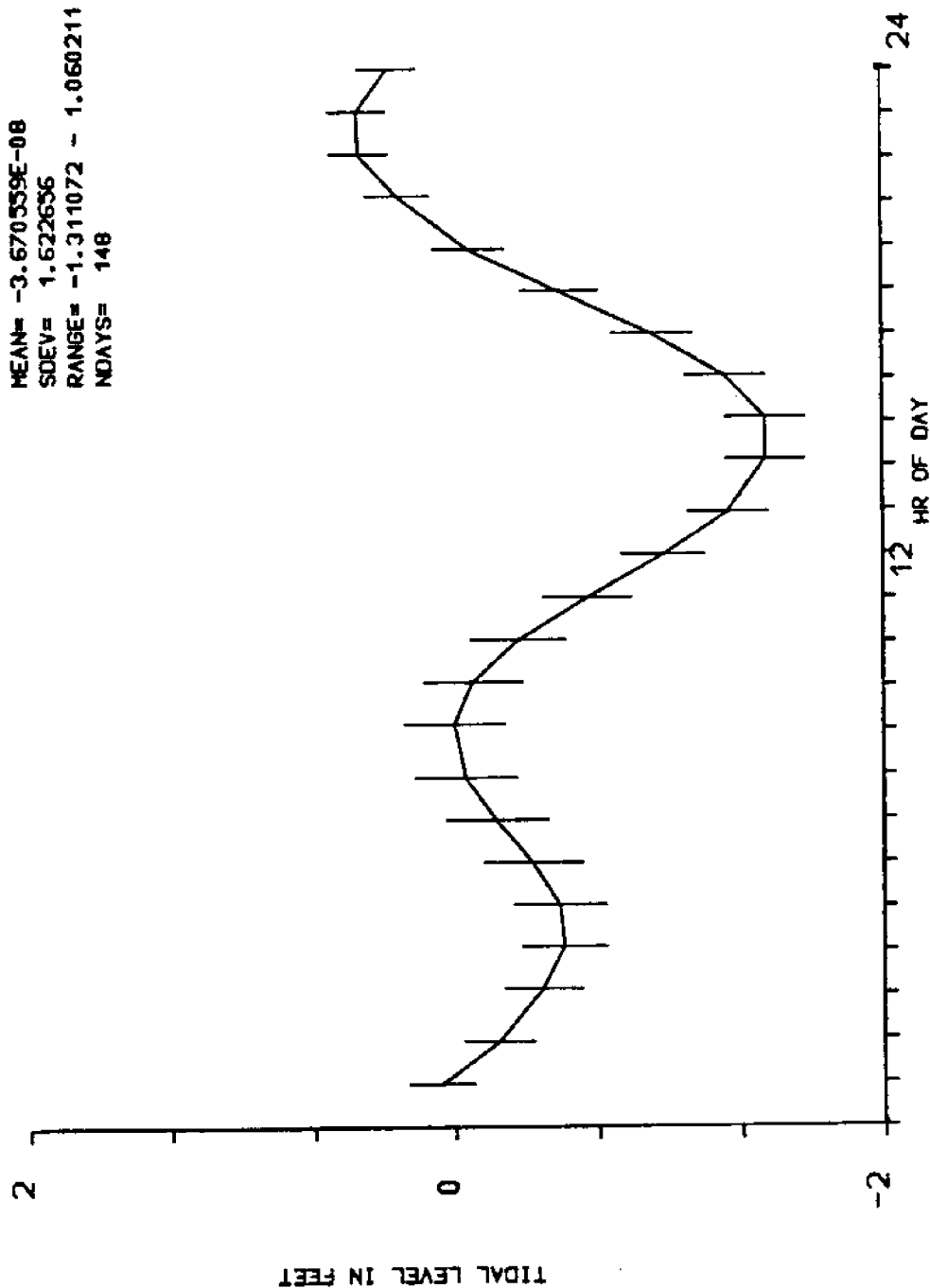


FIGURE 5.2 Averaged cycle of tidal sea surface elevation over a 24 hour day. Produced by averaging all sea surface height from similar times of day over the 113 day deployment period.

EFFECTS ON EFFLUENT FIELD DISTRIBUTIONS

Principal component analysis of the hydrographic data has isolated an effluent component of variability defined by high ammonia and phosphate levels and low salinity and density. Effluent temperatures in the outfall pipes remain nearly constant throughout the year at 20-25 °C (Irwin Haydock, personal communication). These higher than ambient temperatures and very low salinities of the undiluted effluent give it considerable buoyancy (Fischer et al. (1979) estimate a density difference between effluent and seawater of about 0.025 gm/cm³).

The design of the multiport diffusers on the Palos Verdes shelf is such that the effluent should be highly diluted and well mixed with the ambient seawater within a few minutes of exiting the diffuser ports (initial dilutions are estimated at 1:100 or greater). Fischer et al. review the statistics for the two newest and largest of the LACSD outfalls on the Palos Verdes shelf. Their table is reproduced here (Table 5.1), and includes information for the White Point outfalls #'s 3 and 4 which are the only outfalls off White Point which are still used. Although there are considerable variations in the design of these two diffusers they still share many similarities. The diffuser sections are approximately 1000 m long and the ratio of the individual port diameters (on the order of 5-15 cm) to the spacing between the ports (2 m at White Point #4, and 7 m at White Point #3) is more than an order of magnitude. These relatively small ports provide for high discharge velocities of 2-3 m/s which are largely

Summary of Characteristics of Major Pacific Ocean Outfalls (U.S.A.)

Sanitation Districts of	Year operation began	Pipe diameter (inside) (inches)	Length of		Depth of discharge (nominal) (ft)	Design average flow, Q (ft ³ /sec)	Port diameters* (inches)	Port spacing (average) ^b (ft)	Velocity of disch. (nominal) for av. flow (fps)	Q/L (ft ² /sec)	Area factor (total port area/pipe area)
			main outfall (excl. diff.) (ft)	of diffuser, L (ft)							
Los Angeles County	1956	90	7,900	2400	200-210	232	6.5-7.5	24	8	0.097	0.61
White Point No. 3											
City of Los Angeles at Hyperion	1960	144	27,525	7920	195	651	6.75-8.13	48	13	0.082	0.44
San Diego	1963	108	11,500	2688	200-210	363	8.0-9.0 ^c	48	15	0.135	0.39
Sanitation Districts of Los Angeles County											
Whites Point No. 4	1965	120	7,440	4440	165-190	341	2.0-3.6	6	9	0.077	0.51
Metrop. Seattle (West Point)	1965	96	3,050	600	210-240	194	4.5-5.75	3	6	0.323	0.60
Sanitation Districts of Orange County, Calif.	1971	120	21,400	6000	175-195	450	2.96-4.13	12	13	0.075	0.45
Honolulu (Sand Island)	1975	84	9,120	3384	220-235	164	3.00-3.53	12	10	0.048	0.44

* Exclusive of end ports, which are usually somewhat larger.

^b Length of diffuser divided by number of ports; real spacings on each side of the pipe are twice the values indicated.

^c Blocked by orifice plates with openings of 6.5-7 in. for early years' low flow.

TABLE 5.1 Statistics for some large open ocean outfall diffusers, including Los Angeles County White Point No. 3 and No. 4, the two diffusers which operate on the Palos Verdes shelf nearby to the VNMH location. (From mixing in inland and coastal waters, 1979).

responsible for the high initial dilutions. Fischer et al. (1979) provide a number of models to estimate the dilution of a rising buoyant plume. These models must be modified and become more complicated as additional real world complications are added. For example, the individual jets quickly merge and must be considered as a line source of finite length. Then the density stratification variability of the ocean environment must be considered, as well as the current field which will act on the rising plume. All these calculations will be affected by the developing waste field as it perturbs the existing density regime and reduces the effective dilution of effluent discharge with clean seawater.

Beyond the brief period of initial mixing when the high discharge rates cause the effluent jets to entrain surrounding seawater, the further mixing and dilution will be greatly dependent on the ambient density stratification. In an unstratified environment the waste field will rise to the surface. This has advantages in that enhanced additional entrainment and mixing will occur, leading to much greater dilution, but at the same time the waste field may be rapidly transported onshore by winds and surface currents. Studies of surface currents which were made during January and February of 1985 using surface drifters have shown that such relatively rapid (10-30 cm/s) shoreward movements of the surface water do occur off Palos Verdes during the winter (Alan Bratkovich, unpublished data). At the opposite extreme, in a highly stratified environment the waste field may be trapped beneath the thermocline and relatively low dilution rates

achieved due to the fact that bouyant discharge may quickly impinge on the bottom of the already existing waste field where no further effective dilution with clean seawater can take place. This situation can be potentially detrimental in areas of known upwelling where on occasion the near bottom waters will be transported shoreward and then to the surface. Satellite images of sea surface temperature around the Palos Verdes Peninsula suggest that upwelling does frequently occur here (Gary Kleppel, unpublished data).

Temperature gradient estimates between 12 and 34 m at the mooring location show that over this depth range, between January and May of 1985 there was relatively low stratification. The average temperature gradient between 12 and 34 m depth for the four month period was 0.04 °C/m, and the unfiltered (hourly averaged) estimate of temperature gradient commonly goes to zero. The low pass (65 hour filtered) estimate goes very close to zero at two times, once on January 25 and again on February 8. During the hydrographic cruise on January 25 the effluent plume was observed at the surface in the form of a slick lying directly above the diffusers and oriented to the angle at which the diffusers cross the shelf. Confirmation of the presence of the effluent field at the surface was provided by very high ammonia levels above the outfalls during a surface sampling track made across the hydrographic grid along the 60 meter isobath.

Averaged 24 hour cycles, intended to show the typical daily variability of the temperature gradient over the January to May deployment period, suggest that on average the weakest stratification

occurs in the early morning, at about 3 a.m. However the plot of this 24 hour cycle is demeaned by removal of the average for each individual 24 hour period, and in fact the total range of gradients in this figure is only about 0.01 °C/meter, roughly one quarter of the long term average temperature gradient. Because only two points in the water column were used to calculate the temperature gradient the resulting signal must be considered only a rough approximation to the actual vertical stratification conditions.

CONCLUSIONS

During the first four months of 1985, the temperature on the continental shelf near Palos Verdes Peninsula decreased by 2 - 2.5 °C, and only began to increase at the beginning of May. During this same time period, variability in the temperature increased substantially, (monthly temperature variance levels at 12 m went from 0.016 °C² in January to 1.75 °C² in May while at 34 m variance increased from 0.08 °C² to 1.5 °C²) primarily due to tidal frequency contributions to the temperature variance spectrum. The temperature gradient between 12 and 34 m also increased gradually during this time (mean temperature gradients were 0.018 °C/m in January and rose to 0.053 °C/m in May).

Crosscorrelations of demeaned time series of winds with currents, winds with water temperatures and currents with water temperature all drop to low values at time lags of under 6 hours. Only the crosscorrelation of the 12 and 34 m depth temperature records showed high correlation for a significant length of time, (values were above 0.5 at lags of up to 1 week).

Averaged 24 hour cycles produced from time series of the 12 and 34 m depth temperatures, the temperature gradient between them, the currents, winds and the sea surface elevation all show significant features and agreement between different variables. Averaged cycles of cross-shelf and alongshelf components of the wind seem to correlate with the 12 meter depth currents with a lag time of 18 hours. At 34 m the averaged cycle of temperature is about 3 hours out of phase with the averaged cycle of the 34 m cross-shelf current. Based on this

comparison of the averaged daily cycles of temperature and cross-shelf current at 34 m it can be stated that peak onshore currents which occur at 6 a.m. and 5 p.m. correspond to maximum rates of decrease in temperature, and that peak offshore currents at 1 p.m. and midnight correspond to maximum rates of increase in temperature. The situation nearer the surface at 12 m cannot be so clearly developed, probably due to stronger wind and solar affects in a mixed layer which was usually deeper than 12m.

The averaged daily cycle of sea surface elevations nearly mirrors the temperature variation at the 12 and 34 m depths. Highest temperatures in the 24 hour averaged cycles occurred at times of lowest sea surface elevation. With an average temperature gradient of $0.04^{\circ}\text{C}/\text{m}$ and a total range in the 24 hour cycle of sea surface elevations of about 0.6 meters, only about 10% of the observed temperature variation in the daily cycles can be explained as passive vertical movement of the isotherms past the sensors as the sea surface elevation varies. A slight phase shift of the early morning temperature maximum of the cycle at 12 m relative to the cycle at 34 m can be seen as the reason for a minimum in the temperature gradient at 3 a.m. local time. Comparison of the daily averaged current cycles at 12, 23, 34 and 45 m depth indicates the alongshelf current to be relatively constant at all depths and to have only one maximum and minimum in a 24 hour period. The cross-shelf currents have a relatively strong semidiurnal frequency variability near the bottom

and a combination of diurnal and semidiurnal frequency variability near the surface.

Monthly statistics of the alongshelf currents show that there is a weak net current towards the northwest at 23, 34 and 45 m, but that at 12 m in some months the alongshelf current may be to the southeast. Over the entire deployment period however the 12 m current averages to 0.0. Cross-shelf currents at 12, 23 and 34 m have a net onshore component which decreases approximately linearly with depth. Although small, this onshore displacement of water is still unexpected in light of the satellite documented evidence of upwelling off the Palos Verdes Peninsula during the mooring deployment period. This probably reflects a slight rotation of the current components from the 'true' cross-shelf and alongshelf directions, however it also raises the possibility of some consistent variation (in the alongshelf direction) of the cross-shelf current flow patterns.

Historical data sets from nearby inshore CalCOFI stations and from the San Clemente pier provide multiyear averages of the monthly mean temperatures and salinities to be expected in surface waters near the Palos Verdes Peninsula. For the January to May period these records show a net increase in temperature. A mid-winter warming seen by List and Koh (1976) in pier-end data from Southern California is not apparent in our data for January to May 1985, during which time the temperature at the 12 and 34 m sensors dropped by about 2.0 °C. This anomalously cold water is probably due to enhanced upwelling near the peninsula which is suggested by satellite images. Historical data sets

are used to roughly calculate the relative importance of temperature and salinity to the density field. Results show that salinity may be as significant as temperature in defining wintertime density stratification (examination of monthly variance levels of temperature and salinity historical data sets shows an approximately 50% contribution to density by salinity during winter), but in the summer the contribution of salinity to the density field may be an order of magnitude less than that of temperature.

The results of this study can be used to draw several conclusions concerning the effluent field. 1) Daily cycles of the temperature gradient suggest that there is a minimum in the vertical temperature stratification at 3 a.m. 2) Very high levels of tidal scale variability coupled with low crosscorrelations between winds, currents and temperatures, even at very small time lags suggests that reliable generalized current predictor models will be difficult to construct. 3) The tidal frequency variability can complicate the interpretation of spatial maps derived from hydrographic surveys especially during periods of the year when tidal frequency variability in the density field is at its greatest magnitudes (i.e., summer).

REFERENCES

- Anonymous, 1983: Climatic study of the Southern California operating area. Prepared by Naval Oceanography Command Detachment, Asheville, N.C. Prepared under Commander Naval Oceanography Command.
- Bascom, W., 1985: Southern California coastal water research project. Biennial Report, 1983-1984. 331 pp.
- Bendat, J. S. and A. G. Piersol, 1971: Random data: analysis and measurement procedures. Wiley-Interscience, New York 407 pp.
- Bratkovich, A., 1985: Aspects of the tidal variability observed on the southern California continental shelf, J. Phys. Oceanogr., Vol. 15, No. 3, pp. 225-239.
- Cairns, J. L., and K. W. Nelson, 1970: A description of the seasonal thermocline cycle in shallow coastal waters, J. Geophys. Res., Vol. 75, pp. 1127-1131.
- Carslaw, H. S., and J. C. Jaeger, 1959: Conduction of heat in solids. 2nd. ed., Clarendon Press, Oxford.
- Dickey, T. D., and J. J. Simpson, 1982: The influence of optical water type on the diurnal response of the upper ocean, Tellus, Vol. 35B, pp. 142-154.
- Eber, L. E., 1980: Contoured depth-time charts (0 to 200m 1950 to 1966) of temperature, salinity, oxygen and sigma-t at 23 CalCOFI stations in the California Current. CalCOFI Atlas No. 25, 231 pp.
- Fischer, H. B., E. J. List, R. C. Y. Koh, J. Imberger, and N. H. Brooks, 1979: Mixing in Inland and coastal waters. New York, Academic Press Inc. 483 pp.
- Hickey, B., 1979: The California current system - hypotheses and facts, Prog. in Oceanogr., Vol. 8, Pergamon Press, pp. 191-280.
- Howell, T. L., and W. S. Brown, 1985: Nonlinear internal waves on the California continental shelf, J. Geophys. Res., Vol. 90, No. C4, pp. 7256-7264.
- Huyer, A., 1977: Seasonal variation in temperature, salinity, and density over the continental shelf off Oregon, Limnol. Oceanogr., Vol. 22, pp. 442-453.

- Jones, B., A. Bratkovich, T. Dickey, G. Kleppel, A. Steele, R. Iturriaga, and I. Haydock, 1986: Scales of variability in physical, chemical and biological parameters in the vicinity of an ocean outfall. To be presented at the Third International Symposium on Stratified Flows.
- Legendre, L., and P. Legendre, 1983: Numerical Ecology. New York, Elsevier Scientific Publishing Company, 419 pp.
- Liepper, D. F., 1955: Sea temperature variations associated with tidal currents in stratified shallow water over an irregular bottom, J. Mar. Res., Vol. 14, pp. 234-252.
- List, E. J., and R. C. Y. Koh, 1976: Variations in coastal temperatures on the southern and central California coast, J. Geophys. Res., Vol. 81, pp. 1971-1979.
- Lynn, R. J., K. A. Bliss and L. E. Eber, 1982: Vertical and horizontal distributions of seasonal mean temperature, salinity, sigma-t, stability, dynamic height, oxygen and oxygen saturation in the California Current, 1950-1978. Edited by A. Fleminger, CALCOFI Atlas No. 30, Marine Life Research Program, Scripps Institution of Oceanography, La Jolla, California.
- Morrison, D. F., 1976: Multivariate Statistical Methods. McGraw-Hill, New York. 415 pp.
- Nelson, C. S., and D. M. Husby, 1983: Climatology of surface heat fluxes over the California current region. NOAA Technical Report NMFS SSRF-763, US Department of Commerce. 155 pp.
- Pickard, G. L., 1963: Descriptive physical oceanography. Pergammon Press, Oxford. 200 pp.
- Pond, S., and G. L. Pickard, 1983: Introductory dynamical oceanography. 2nd. Ed. New York, Pergammon Press, 329 pp.
- Robinson, M. K., 1972: Surface water temperatures at shore stations, U.S. west coast and Baja California, 1964-1972, Scripps Inst. of Oceanogr., La Jolla, Calif.
- Smith, R. C., and K. S. Baker, 1978: The bio-optical state of ocean waters and remote sensing, Limnol. Oceanogr., Vol. 23(2) pp. 247-259.
- Stommel, H., K. Saunders, W. Simmons, and J. Cooper, 1969: Observations of the diurnal thermocline, Deep-Sea Res., Supplement Vol. 16, pp. 269-284.

- Tsuchiya, M., 1980: Inshore circulation in the Southern California Bight, 1974-1977, Deep-sea Res., Vol. 27A, pp. 99-118.
- Winant, C. D., 1983: Longshore coherence of currents on the southern California shelf during the summer, J. Phys. Oceanogr., Vol. 13, No. 1, pp. 54-64.
- , and A. Bratkovich, 1981: Temperature and currents on the southern California shelf: A description of the variability, J. Phys. Oceanogr., Vol. 11, pp. 71-86.

APPENDIX

Principal Component Analysis Review

Principal component analysis is a powerful multivariate statistical technique used to summarize trends in data sets. It is particularly well suited to situations involving large numbers of variables. Variables which are affected similarly by the same processes will correlate with one another and will form a component reflecting that interaction. A loading value can be calculated for each variable which shows how closely it is related to each of the principal components. Calculated Principal Component scores represent the relative magnitude of the different components.

Procedure:

- 1) Calculate the normalized covariance matrix (correlation matrix).
- 2) Determine the eigenvalues of the covariance matrix, (This provides the variance associated with each eigenvector or component).
- 3) Calculate factor loadings (these are the coefficients for each of the eigenvectors and show the relationship between variables and calculated principal components).
- 4) Calculate the principal component scores.

An example of principal component analysis is shown below. The data used is a subset of the data used in the analysis done by Burton Jones for the SG/LAC hydrographic data from January 28, 1985. In this example three variables are used, temperature, chlorophyll and ammonia. These three variables were sampled at 0, 10, 20, 30, 40 and

50 m at two stations (X=0, and X=2 on the Y=0 line, see figure 1.1 for locations). A correlation matrix was prepared using the formula below to determine correlation values;

$$R_{k,l} = \frac{\sum (X^2_{i,k} * X^2_{i,l})}{\sum X^2_{i,k} * \sum X^2_{i,l}} \quad \begin{array}{l} i = \text{sample \#}. \\ k,l = \text{variable \#'s}. \end{array} \quad (1)$$

The resulting correlation matrix of temperature, chlorophyll and ammonia looks as follows;

$$R = \begin{bmatrix} 1.000 & 0.742 & 0.725 \\ 0.742 & 1.000 & 0.344 \\ 0.725 & 0.344 & 1.000 \end{bmatrix}$$

Eigenvalues and eigenvectors can be calculated from this correlation matrix using the following relationship;

$$R \cdot V = E \cdot V \quad (2)$$

where R = the correlation matrix.

E = an eigenvalue.

V = the eigenvector corresponding to each eigenvalue.

For this example the above relationship becomes;

$$\begin{bmatrix} 1.000 & 0.742 & 0.725 \\ 0.742 & 1.000 & 0.344 \\ 0.725 & 0.344 & 1.000 \end{bmatrix} \cdot \begin{bmatrix} X \\ Y \\ Z \end{bmatrix} = E \cdot \begin{bmatrix} X \\ Y \\ Z \end{bmatrix}$$

This can be rewritten in equation form as;

eigenvalue;

Eigenvectors:	-0.646	0.010	-0.763	temperature
	-0.543	0.697	0.469	chlorophyll
	-0.534	-0.717	0.445	ammonia

The Eigenvalues give the variance associated with each component. Hence the percent of variance accounted for by each eigenvector is given by:

$$E_i / (\sum E_i) * 100\% \quad (11)$$

% of variance: 74% 22% 4%

For analysis of more than three variables numerical methods are needed to calculate the eigenvalues and eigenvectors.

These results tell us that 74% of the variance in the data is in the first component, 22% is in the second component, and 4% is in the third component.

The scores, or value of each principal component for each observation can then be calculated with the following equation:

$$S_{i,j} = \frac{\sum (X_{i,k} - \bar{X}_k / s_k) \cdot F_{j,k}}{Eig_j} \quad (12)$$

where i = sample #.	Eig _j = Eigenvalue of component j.
j = principal component #.	X _{i,k} = Value of variable.
k = variable #.	F _{j,k} = Loading of variable k on component j.

Additional information on principal component analysis can be found in Legendre and Legendre (1983), and Morrison (1976).